The tectonic and rheological evolution of an attenuated cross section of the continental crust: Ivrea crustal section, southern Alps, northwestern Italy and southern Switzerland

M. R. HANDY *Geologisches Institut, Universität Bern, Baltzerstrasse 1, 3012 Bern, Switzerland*
A. ZINGG *Geologisches Institut, Universität Basel, Bernoullistrasse 32, 4056 Basel, Switzerland*

ABSTRACT

The tectonic and rheological evolution of the southern Alpine continental crust is reconstructed from structural, petrological, and radiometric studies in the Ivrea and Strona-Ceneri basement units. The deep crust of the southern Alps acquired its present compositional and metamorphic zonation during Paleozoic magmatism and amphibolite-to granulite-facies regional metamorphism. Inferred strength contrasts between lower crustal and upper mantle rocks in the Ivrea zone are low at the high temperatures of regional metamorphism. Late Paleozoic transtension and basic to intermediate magmatism in all crustal levels preceded extensional faulting associated with the formation of a passive continental margin during early Mesozoic time. Extensional uplift and cooling of the basement section is coupled with crustal-scale trends of increasing rheological stratification, grain size reduction, and strain localization. Mylonitic shear zones in the lower crust and a broad zone of noncoaxial shear at the base of the intermediate crust in the Ivrea zone are inferred to have controlled the high-strain rheology of the attenuating southern Alpine crust. The deep crust in the thinned Ivrea crustal cross section transferred noncoaxial strain from the upper mantle to the intermediate and upper crust. Final uplift and exposure of the deep southern Alpine crust occurred during Late Cretaceous to Tertiary Alpine thrusting.

INTRODUCTION

Much of what is currently known about lithospheric rheology stems from a combination of geophysical surveys (reviews in Barazangi and Brown, 1986; Mooney and Brocher, 1987) and laboratory experiments on rocks and minerals designed to simulate physical conditions in the lithosphere (Carter, 1976; Tullis, 1979; Kirby, 1983; Carter and Tsenn, 1987). The correlation of experimentally predicted strength-depth profiles and deformational modes with crustal seismicity is generally consistent with the concept of a compositionally and rheologically stratified continental lithosphere (Brace and Kohlstedt, 1980; Kirby, 1980; Meissner and Strehlau, 1982; Sibson, 1982, 1983; Smith and Brun, 1984; Ranalli and Murphy, 1987). Existing models adequately describe low-strain intraplate rheology (for example, Kuznir and Park, 1986), but lithospheric rheology at active plate margins is much more complex due to changing thermobarometric conditions during deformation as well as to the marked lithological and structural heterogeneity in the crust prior to deformation.

The Ivrea crustal cross section in northwestern Italy and southern Switzerland (Fig. 1) is an excellent area to test geophysical models of the continental crust. The section actually consists of two basement units, the Ivrea zone and the Strona-Ceneri zone, which represent thinned lower to intermediate continental crust of the southern Alps (reviews in Zingg, 1983; Boriani and Origoni Giobbi, 1984; Zingg and others, 1990). The Permian-Mesozoic sedimentary cover of the Strona-Ceneri zone crops out to the south of the basement section (Fig. 1). The history of the Ivrea and Strona-Ceneri zones is loosely subdivided into three tectonometamorphic episodes (Fig. 2). Large-scale magmatism and regional metamorphism during the Paleozoic era (episode 1) are responsible for the general compositional and metamorphic zonation presently observed in the crustal section. Crustal attenuation and rifting during late Paleozoic and early Mesozoic time (episode 2) thinned the crust to a thickness of 10 to 20 km and brought the basement section to shallower crustal levels. The final emplacement and steepening of the Ivrea crustal section in the upper crust (episode 3) resulted from polyphase Alpine transpressional tectonics (Laubscher, 1971; Schmid and others, 1987).

We use a combination of structural, petrologic, and radiometric information to reconstruct the tectonic and rheological evolution of the Ivrea crustal cross section. The main purpose is to show how the kinematic and thermal history of the continental crust is linked to its high-strain rheology. The deep crustal pre-Alpine structures and high-grade metamorphism are remarkably well preserved in the Ivrea and Strona-Ceneri zones because the obliterating effects of Alpine metamorphism and penetrative deformation are restricted to the Insubric line and to the Penninic and Austro-Alpine basement nappes to the north and west (Fig. 1). Alpine folds and faults transect the crustal section and modify the original crustal configuration (Fig. 1), but these structures do not disrupt the general continuity among the different crustal levels.

Figure 1. Tectonic map of the Ivrea crustal cross section and neighboring units in the western part of the southern Alps. Movement sense of faults compiled from Bertotti (1990), Handy (1987), Schmid and others (1987), and our own observations.

Geological Society of America Bulletin, v. 103, p. 236–253, 11 figs., February 1991.

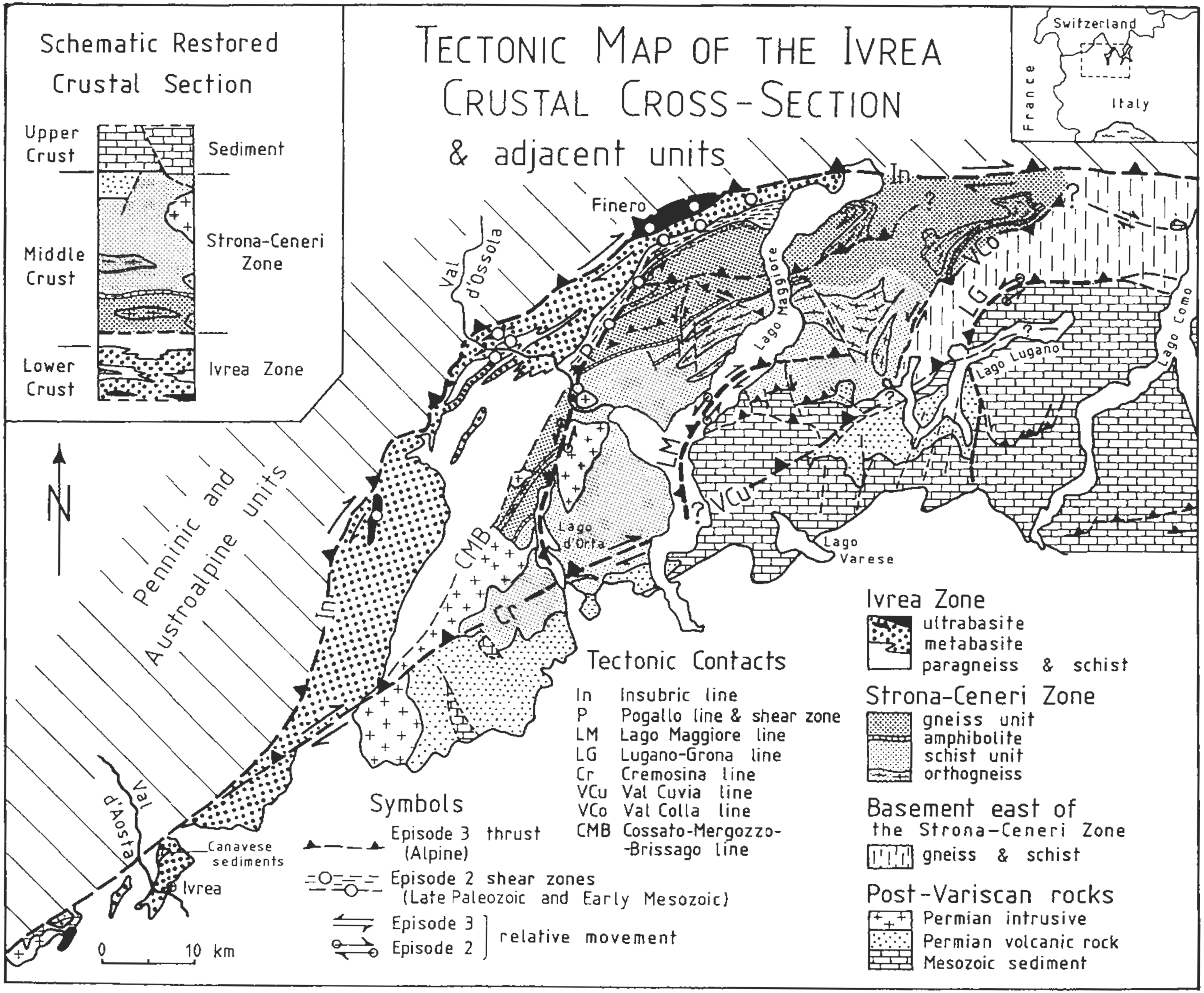

Tectonic Map of the Ivrea Crustal Cross-Section & adjacent units
Schematic Restored Crustal Section
Upper Crust
Sediment
Middle Crust
Strona-Ceneri Zone
Lower Crust
Ivrea Zone
Switzerland
France
Italy
N
Penninic and Austroalpine units
Finero
Val d'Ossola
Lago Maggiore
Lago Lugano
Lago Como
Lago d'Orta
Lago Varese
Val d'Aosta
Canavese sediments
Ivrea
0 10 km
In
P
LM
LG
VCo
VCu
CMB
Cr
Tectonic Contacts
In Insubric line
P Pogallo line & shear zone
LM Lago Maggiore line
LG Lugano-Grona line
Cr Cremosina line
VCu Val Cuvia line
VCo Val Colla line
CMB Cossato-Mergozzo--Brissago line
Symbols
Episode 3 thrust (Alpine)
Episode 2 shear zones (Late Paleozoic and Early Mesozoic)
Episode 3
Episode 2
relative movement
Ivrea Zone
ultrabasite
metabasite
paragneiss & schist
Strona-Ceneri Zone
gneiss unit
amphibolite
schist unit
orthogneiss
Basement east of the Strona-Ceneri Zone
gneiss & schist
Post-Variscan rocks
Permian intrusive
Permian volcanic rock
Mesozoic sediment

EPISODE	AGE	EVENTS	FABRICS	EVENTS	FABRICS
			high-pressure/low-temperature event: age and extent unknown		
Episode 1: Crustal genesis and orogenesis	PALEOZOIC	polyphase deformation, amphibolite to granulite facies regional metamorphism, anatexis	annealed medium to coarse grained	Ordovician granitoids polyphase folding and shearing, amphibolite facies regional metamorphism, anatexis	annealed fine to coarse grained (annealed mylonitic fabrics)
			Late Paleozoic magmatic activity in all crustal levels		
Episode 2: Overall cooling and crustal attenuation	PERMIAN - ? TRIASSIC ?	high-temperature shearing	mylonitic locally annealed	SW-rim of the Strona-Ceneri zone: erosion and transtensional faulting	cataclastic
	TRIASSIC - LIASSIC	retrograde amphibolite and greenschist facies shearing (Pogallo shear zone)	mylonitic, locally cataclastic	NW-rim of the Strona-Ceneri zone: localized retrograde lower amphibolite to greenschist facies shearing (extensional faulting in shallower crustal levels, e.g. sediments)	mylonitic, locally cataclastic cataclastic
Episode 3: Alpine transpressional tectonics	CRETACEOUS - TERTIARY	formation of the geophysical Ivrea body steepening of the Ivrea crustal section, localized folding and thrusting	cataclastic	localized thrusting, folding and strike-slip faulting under anchizone conditions or lower	cataclastic
		NW-rim of the Ivrea zone: greenschist facies shearing along the Insubric line	mylonitic		
		I V R E A Z O N E		S T R O N A - C E N E R I Z O N E	

Figure 2. Tectonometamorphic history of the Ivrea and Strona-Ceneri basement units.

STRUCTURAL STYLE AND INFERRED RHEOLOGY

A Field and Microscopic Approach to Rheology

The magnitude, distribution, and style of strain are used to infer the competence contrast among different rocks and minerals. We note at the outset that most of our structural observations come from the central to northeastern part of the Ivrea and Strona-Ceneri zones (between the Val d'Ossola and the northeastern end of the Lago Maggiore, Fig. 1). This informational bias also reflects the general distribution of published structural work in the area.

Broad constraints on the relative viscosity of different rock layers are obtained by applying experimental and theoretical relationships in deformed viscous materials to natural structures. For buckled layers with similar initial thickness that undergo comparable strains, decreasing viscosity contrast is associated with a successive change in the fold style from parallel to concentric to similar to ptygmatic (Fig. 3a; Ramsay, 1967). At very high strains, fold amplitude increases and the style becomes increasingly similar to ptygmatic, irrespective of the initial fold form. The viscosity contrast between composite layers can be expressed as (after Biot, 1964; Ramberg, 1964)

$$\frac{\eta_a}{\eta_b} = \frac{(W_d/2\pi t)^3}{n}, \tag{1}$$

where η_a and η_b are, respectively, the viscosities of the competent and incompetent layers, W_d is the predominant fold wavelength, t is the average thickness of the competent layer, and n is the number of layers. For bulk extensional deformation, barrel-shaped boudins or porphyroclasts in a weak matrix generally form in experimentally deformed materials with a viscosity contrast between constituent phases of an order of magnitude or greater (for example, Jordan, 1987). At lower relative viscosities, the boudin shape is highly strain dependent, and the more competent material tends to form lenticular boudins and pinch-swell structures within the plane of flattening (Fig. 3a; Ramsay, 1967). The mineral or minerals that accommodate most of the strain in a rock are inferred to govern its bulk strength. Identifying the micromechanisms of flow in these minerals (microstructural criteria in Knipe, 1989) allows us to estimate the rheology of the rock.

Despite the obvious limitations of this approach (poor constraints on strain and strain rate, locally inhomogeneous deformation), structures are reliable qualitative to semiquantitative indicators of rheology once their age and regional kinematic significance are known. The age of structures in different levels of the Ivrea crustal cross section is constrained by correlating the syn-, inter-, and postkinematic conditions of metamorphism with the radiometrically determined temperature-time curves for different parts of Ivrea and Strona-Ceneri zones in Figure 4.

Deformation during Regional Metamorphism (Episode 1)

Regional metamorphism generally increases across the crustal section from amphibolite facies in mica schist, paragneiss, and orthogneiss of the Strona-Ceneri zone to granulite facies in interlayered paragneiss and metabasic and ultrabasic rocks in the northwestern part of the Ivrea zone. At least two phases of folding affected the Ivrea and Strona-Ceneri rocks during regional metamorphism (Figs. 3b and 3c). Early isoclinal to ptygmatic folds with amplitudes on the centimeter to multimeter scale preceded open to close, similar folds with amplitudes on the centimeter (Figs. 3d–3f) to kilometer scale (Schmid, 1967; Steck and Tièche, 1976). Episode 1 structures in the Ivrea and Strona-Ceneri zones indicate the following sequence of increasing flow strength: schist < paragneiss < metabasite ≅ peridotite < pyroxenite. The predominance of boudinage structures with moderate to high aspect ratios (Figs. 3g–3i) suggests that high-grade regional metamorphism in the intermediate to lower continental crust is associated with low strength contrasts among all rocks. In addition, the observations indicate the importance of grain size as a determinant of relative flow strength at high strains (Fig. 3h and discussion in next section).

Episode 1 microstructures are strongly annealed under the conditions of regional metamorphism. This annealing obscures most traces of the microrheological behavior (Figs. 5a–5c). The best examples of episode 1 microstructures come from metabasic and ultrabasic rocks, because they are less affected by episode 2 shearing than are paragneiss and schist. Thermal equilibration of the microstructures (straight grain boundaries and stable grain-boundary triple junctions) is generally more complete in the metagabbro than in the peridotite (Kruhl and Voll, 1978/79), suggesting that the olivine in peridotite was somewhat weaker (that is, flowed more and/or longer) than the feldspar-amphibole-pyroxene aggregates in metagabbro.

Migmatites are frequently observed in the transitional region between intermediate and lower crust in the Ivrea crustal cross section, that is, within upper-amphibolite–facies paragneiss and locally along the contact between paragneiss and metabasite (Schmid and Wood, 1976; Zingg, 1980). Unfortunately, the strong anneal of the rocks makes it impossible to establish whether or not melt-enhanced movement occurred. Certainly, partial melt layers do not appear to offset rock series with different lithological, metamorphic, or radiometric characteristics. Syntectonic anatexis has been proposed to explain intracrustal detachment in other Variscan terrains of central Europe (Eisbacher and others, 1989), but in the Ivrea crustal section, field evidence for regionally significant melt-enhanced shearing during the Paleozoic remains equivocal.

When assessing the rheological significance of episode 1 structural style across the crustal section, it is important to realize that the Ivrea and Strona-Ceneri zones may have occupied laterally different tectonic positions in the crust during at least part of the Paleozoic. The Ivrea zone contains coaxial, predominantly northeast-plunging folds and associated intersection and stretching lineations (Schmid, 1967; Kruhl and Voll, 1976; Steck and Tièche, 1976), whereas the folds and lineations in the Strona-Ceneri zone trend and plunge variably (Boriani and others, 1977) owing to the interference of multiple folding events (Handy, 1987). The discrepancy in episode 1 fold and lineation orientations between the Ivrea and Strona-Ceneri zones may reflect primary differences in the Paleozoic tectonic evolution of the two basement units in addition to the modifying effects of later episode 2 shearing concentrated within the structurally deeper Ivrea zone. Moreover, the entire contact between the Ivrea and Strona-Ceneri zones is tectonic according to Boriani and Sacchi (1973), and the divergent radiometric temperature-time paths on either side of this contact (Fig. 4a) suggest that it may have accommodated substantial Paleozoic thrusting and thickening prior to episode 2 extensional shearing. The Paleozoic kinematic framework in the Alps is obscured by the early Mesozoic and Alpine overprint, but local geochemical (basic rocks with oceanic affinity) and petrological (high-P/low-T relics) data support the view that the Ivrea zone was located within a convergent margin during early Paleozoic time (Sills and Tarney, 1984) and that crustal shortening affected both the Ivrea and Strona-Ceneri zones during the Variscan orogeny (for example, Boriani and others, 1977).

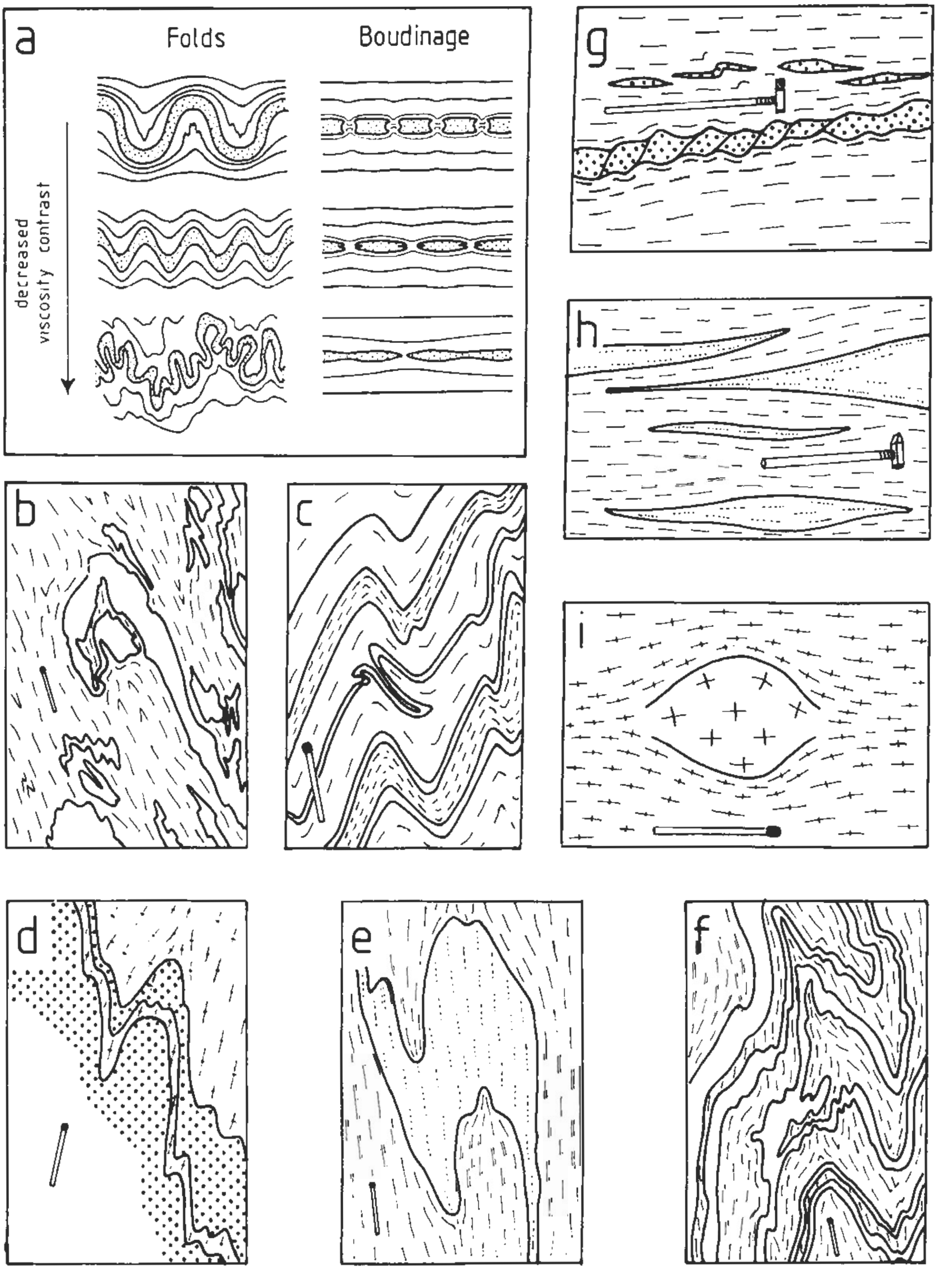

Crustal Attenuation, Magmatism, and Rifting (Episode 2)

Deformation of the southern Alpine basement during episode 2 involved mylonitic shearing combined with an overall transition from high temperatures (600–900 °C) to low temperatures (<300 °C) in the Ivrea zone (Figs. 4a and 4b). The successive closure of mineral isotopic systems documenting this late Paleozoic to early Mesozoic thermal transition probably represents the superposition of thermal regimes related to different regional tectonic events that are more readily differentiated in the upper crust of the southern Alps. We tentatively distinguish two stages of

Figure 3. Episode 1 structures.
(a) Dependence of fold and boudinage styles on viscosity contrast between layers.
(b) Refolded fold in migmatitic (?) feldspathic layer (white) within paragneiss in the amphibolite-facies part of the Ivrea zone.
(c) Two generations of folds in a quartz layer (white) within an amphibolite-facies paragneiss of the Strona-Ceneri zone.
(d) Folded contact between pyroxenite (stippled) and phlogopite-bearing peridotite (dashed schistosity) in the granulite-facies part of the Ivrea zone.
(e) Ptygmatically folded amphibolite layer (dotted schistosity) within a paragneiss (dashed schistosity) in the amphibolite-facies part of the Ivrea zone. Amphibolite was more competent than was paragneiss.
(f) Folded feldspathic layers (white) and amphibolitic layers (dashed) showing that amphibolite was slightly less competent than was feldspar rock.
(g) Asymmetrically rotated boudins of competent pyroxenite (stippled) within metagabbro (dashed schistosity) in the granulite-facies part of the Ivrea zone.
(h) Attenuated amphibolite layers (dotted schistosity) within amphibolite-facies paragneiss (dashed schistosity) in the Strona-Ceneri zone.
(i) Coarse-grained olivine augen within fine-grained, foliated peridotite in the granulite-facies part of the Ivrea zone. Coarse-grained olivine is more competent than is fine-grained olivine.
Scale match in b–f and i is 3 cm long; hammer in g and h is 55 cm long.

episode 2 tectonism (Fig. 2): (1) a late Paleozoic to Early Triassic stage of high-temperature mylonitization in the lower crust that is contemporaneous with widespread basic to intermediate magmatism in all crustal levels and with the opening of east-northeast–west-southwest–trending "Collio-Verrucano" basins (Cassinis and others, 1978) in the upper crust and (2) a Middle Triassic to Early Jurassic stage of high- to low-temperature extensional shearing associated with east-west–directed rifting prior to active spreading of the Tethyan ocean (Bernoulli and others, 1979; Winterer and Bosellini, 1981). We hasten to emphasize, however, the difficulty in establishing an unequivocal temporal distinction between these two stages in the basement based solely on the correlation of radiometric thermal history with microstructures (discussion in Brodie and Rutter, 1987, p. 209; Zingg and others, 1990; and below).

The deformational style during episode 2 reveals that the competence contrasts among rocks and minerals are much more pronounced than during episode 1. Strain in lower crustal peridotite, metabasite, and granulite-facies paragneiss (stronalite) is localized within mylonite zones that range in width from a few centimeters to as much as 10 m (references in Fig. 6a). These mylonite zones usually display sharp, discordant to concordant boundaries with the foliation in the adjoining rock. The strong anneal in the rock outside the shear zones and the difficulty in distinguishing annealed microfabrics of episodes 1 and 2 make it hard to determine how much strain, if any, was accommodated outside these shear zones during episode 2. Deflection of the host-rock foliation adjacent to the mylonites generally occurs within a broader zone in metabasite than in peridotite. Kruhl and Voll (1978/79, p. 105) observed that the amphibolite-facies deformation of metabasite is penetrative, but that peridotite behaves more rigidly and is penetrated only by very discrete ultramylonitic shear zones. Deformation is very diffuse in the relatively hydrous middle- to upper-amphibolite–facies paragneiss and schist (kinzigites) at the originally shallower southeastern margin of the Ivrea zone. These relations indicate that quartz-rich paragneiss was weaker than metabasite and peridotite during episode 2 deformation.

Most rocks affected by episode 2 shearing show syntectonic grain size reduction of their constituent minerals. This involves a combination of dynamic recrystallization, cataclasis, and syntectonic metamorphic reaction. Which one of these deformation mechanisms dominates depends on the mineralogy of the host rock and on the conditions of deformation. The viscous creep of metabasite, paragneiss, and most peridotite sheared under upper-amphibolite–facies conditions is governed by the creep of the same minerals as in the less-deformed rock adjacent to the mylonite zones (Fig. 6a). Grain size reduction in these minerals primarily involves dynamic recrystallization with no or only minor compositional changes between host grains (clasts) and the fine recrystallized grains in the mylonitic matrix (Brodie, 1980, 1981). In contrast, the creep of retrograde upper-amphibolite–facies mylonite in phlogopite-bearing peridotite and the creep of retrograde greenschist-facies mylonite in paragneiss at the Pogallo line are controlled by very fine-grained, micaceous reaction products (Figs. 6a and 6b).

The mineralogical and compositional evidence from the shear zones (Fig. 6a) indicates that high-temperature mylonitization in the originally deep crustal parts of the Ivrea zone generally occurred at temperatures lower than, or at least comparable to, those attained during episode 1 amphibolite- to granulite-facies regional metamorphism (Zingg, 1983; discussion in Zingg and others, 1990). Some metabasic and peridotitic shear zones contain annealed matrix grains and mineral reactions under static conditions (Fig. 6a), indicating that locally at least, high temperatures outlasted mylonitization. To the extent that chemical equilibrium was established during shearing, localized prograde mylonitization reported for some metabasic rocks (Brodie, 1981) may result from conductive heating of the hanging wall of extensional allochthons within the lower crust (Brodie and Rutter, 1987).

The microstructures and inferred rheology of mylonitized high-grade paragneiss in the lower crust depend strongly on the relative proportions of quartz and feldspar and on the syntectonic grain size of these minerals. Generally, quartz undergoes dynamic recrystallization at lower strains than does feldspar, which forms clasts in the fine-grained quartz matrix (Fig. 7a; see also Figs. 36 and 37 in Schmid, 1967). Quartz thus accommodates most of the strain and is inferred to govern viscous flow of most paragneiss, even in rocks with as little as 20 vol. % quartz (Handy, 1990). The dynamically recrystallized grain size of quartz in some mylonitized high-grade paragneiss is very small (<20 μm), smaller than or comparable to that of quartz from greenschist-facies mylonite along the Pogallo line (~ 20 μm; inset to Fig. 8). Comparison of such fine, dynamically recrystallized quartz grain sizes in high-grade mylonite with laboratory-calibrated piezometers (review in Ord and Christie, 1984) indicates that very high flow stresses prevailed despite the high temperature of deformation ($\sigma >100$ MPa at ~ 600 °C). Quite possibly, the fine recrystallized grain size reflects the lower water activity in quartz within the originally granulite-facies rocks. Dynamically recrystallized feldspar is even finer grained (<10 μm)

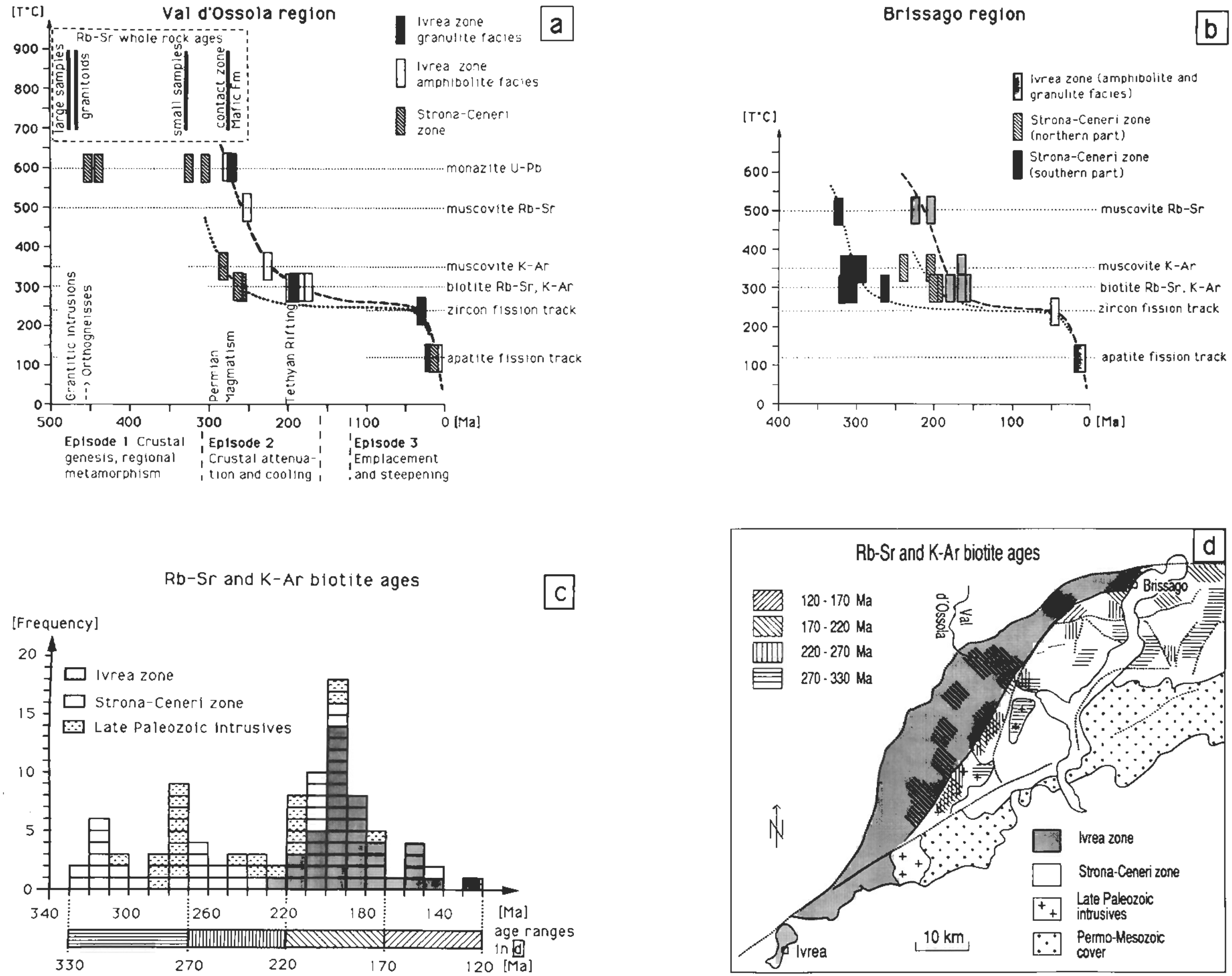
Val d'Ossola region
a
Ivrea zone granulite facies
Ivrea zone amphibolite facies
Strona-Ceneri zone
Rb-Sr whole rock ages
large samples
granitoids
small samples
contact zone
Mafic Fm
monazite U-Pb
muscovite Rb-Sr
muscovite K-Ar
biotite Rb-Sr, K-Ar
zircon fission track
apatite fission track
Granitic intrusions --> Orthogneisses
Permian Magmatism
Tethyan Rifting
[T°C]
[Ma]
Episode 1 Crustal genesis, regional metamorphism
Episode 2 Crustal attenuation and cooling
Episode 3 Emplacement and steepening
Brissago region
b
Ivrea zone (amphibolite and granulite facies)
Strona-Ceneri zone (northern part)
Strona-Ceneri zone (southern part)
muscovite Rb-Sr
muscovite K-Ar
biotite Rb-Sr, K-Ar
zircon fission track
apatite fission track
[T°C]
[Ma]
Rb-Sr and K-Ar biotite ages
c
[Frequency]
Ivrea zone
Strona-Ceneri zone
Late Paleozoic intrusives
[Ma]
age ranges in d
[Ma]
Rb-Sr and K-Ar biotite ages
d
120 - 170 Ma
170 - 220 Ma
220 - 270 Ma
270 - 330 Ma
Val d'Ossola
Brissago
Ivrea
N
10 km
Ivrea zone
Strona-Ceneri zone
Late Paleozoic intrusives
Permo-Mesozoic cover

Figure 4. Temperature-time curves for the central (a) and northeastern (b) parts of the Ivrea and Strona-Ceneri zones constructed with whole-rock and mineral ages from the literature. Mineral ages interpreted as cooling ages. Frequency versus age histogram for biotite (c) shows the four intervals of biotite ages in the Ivrea crustal cross section that are plotted as age domains on the generalized geologic map in d. Note the general decrease in biotite ages with increasing paleo-depth (from southeast to northwest) across the basement section. The biotite age pattern in d reflects cooling during late Paleozoic to early Mesozoic extensional uplift and subsequent exposure of different crustal levels during Alpine thrusting (see text). Radiometric ages compiled and discussed in Zingg (1983) and Boriani and others (1985). Fission-track ages from Wagner and others (1977) and Hurford (1986); recent (post-1985) age determinations from Pinarelli and others (1988) and Bürgi and Klötzli (1990).

than quartz and forms extremely long clast tails within the quartz matrix (Fig. 7b). Thus, at high strains, dynamic recrystallization of the initially much stronger feldspar is associated with a reduction in the relative viscosity of feldspar and quartz to near unity. A similar development is reported elsewhere in mylonites deformed at granulite-facies and retrograde amphibolite-facies conditions (Boullier and Gueguen, 1975; Behrmann and Mainprice, 1987) and may reflect the activity of grain-size–sensitive creep mechanisms in the feldspar aggregates.

Crustal shearing that postdates late Paleozoic magmatism is concentrated within a 1- to 3-km-wide shear zone (the Pogallo shear zone; Handy, 1987). This crustal-scale shear zone primarily affects quartz-rich, amphibolite-facies paragneiss and schist at the originally shallower, southeastern margin of the Ivrea zone (Figs. 1 and 8). Pogallo-aged shearing also affected granulite-facies paragneiss, metabasite, and peridotite in the Ivrea zone, and distinguishing the initial stages of Pogallo mylonitization from Early Permian extensional shearing in these high-grade rocks is difficult, if not impossible (discussion below). The deformation involved diffuse, inhomogeneous shearing under retrograde amphibolite-facies conditions in the bulk of the shear zone and hydrous greenschist-facies mylonitization (the Pogallo line) along part of the cooler southeastern rim of the Ivrea zone, adjacent to the Strona-Ceneri zone. Strike-parallel trends from southwest to northeast within the Pogallo shear zone of (1) progressively higher-grade syntectonic mineral assemblages, (2) increased syntectonic grain boundary migration recrystallization in quartz, and (3) coarser dynamically recrystallized quartz grain size (Fig. 8 in Handy, 1987) suggest that the Pogallo shear zone was a dipping shear zone, with its deepest parts presently exposed at the northeastern end of the Lago Maggiore (Figs. 1 and 8). Kinematic indicators show that Pogallo shearing uplifted and displaced the Ivrea zone to the southwest with respect to the Strona-Ceneri zone in present-day coordinates (asymmetry of quartz c-axis patterns in Fig. 8; Fig. 13 in Handy, 1987). Schmid and others (1987) have proposed that Neogene backthrusting along the Insubric line caused folding and steepening of the intermediate to lower crustal levels of the Ivrea

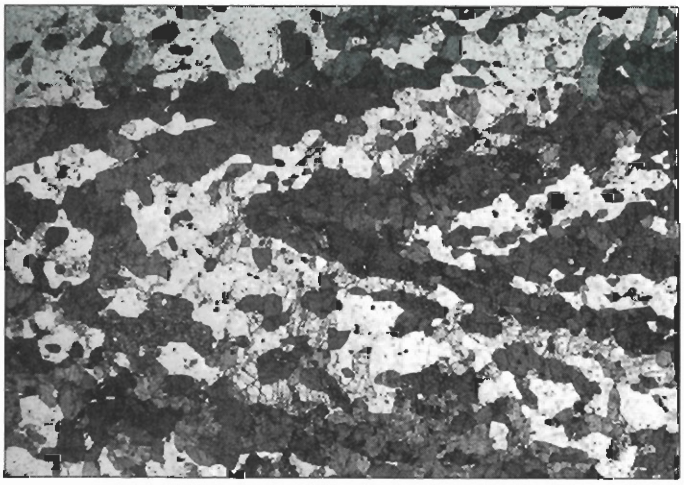
a

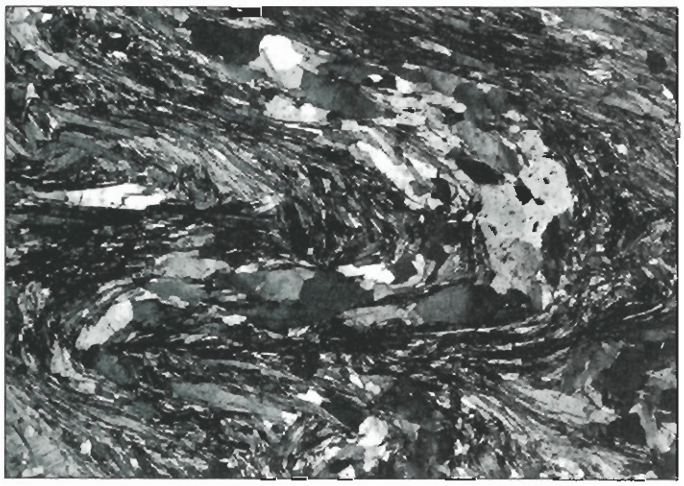
b

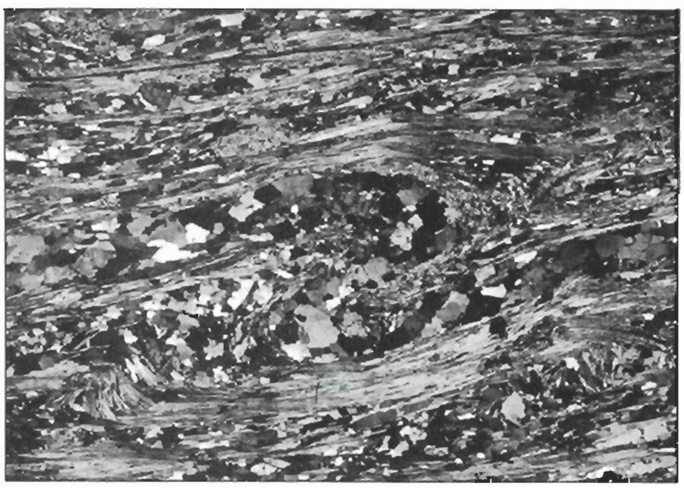
c

Figure 5. Episode 1 microstructures.

(a) Statically recrystallized amphibole (dark pleochroic layers) and plagioclase (light nonpleochroic layers) define the hinge zone of a close fold in a metabasite from the amphibolite-facies part of the Ivrea zone (plane light; frame length, 11.5 mm).

(b) Annealed microstructure in isoclinally folded paragneiss from the amphibolite-facies part of the Ivrea zone (polarized light; frame length, 11.5 mm).

(c) Annealed microstructure in isoclinally folded, medium-grained Strona-Ceneri granitic gneiss (polarized light; frame length, 11.5 mm).

PROTOLITH			HIGH TEMP. SHEAR ZONES						a
			porphyroclasts			mylonitic matrix		metamorphism	
rock type & mineral	mode (vol %)	grain size (mm)	intragranular strain features	grain shape	inferred deformation mechanisms	grain size (µm)	inferred deformation mechanisms	syntectonic to post-tectonic reactions/ local annealing* and minor changes in composition**	references
PERIDOTITE									
olivine	58	2.2	U, B	A (R)	DC	80, < 30	<u>DC</u>, GS	olivine* → orthopyroxene + spinel	Garuti & Friolo (1978/79): Fig. 6
orthopyroxene	22	1.4	U, F, B	E (A)	DG, CA	< 10	GS	exsolution lamellae, new grains rare	Kruhl & Voll (1978/79)
clinopyroxene	11	1.4	U, F, B	E (A)	DG, CA	< 10	GS	clinopyroxene* → phlogopite**	Brodie (1980): Fig. 1
amphibole	3	1.4	U, B, F	I	DG, CA			amphibole* → phlogopite**	Rutter & Brodie (1988): Fig. 6
phlogopite	2	1.0	U, B	I	DG, CA	< 30	<u>GS</u>		Handy (1989): Fig. 11
other	4	0.3							
METABASITE									
plagioclase	46	1.0	U, B, F	A, R	DC	80, < 20	<u>DC</u>	* and often **	Walter (1950): many Figs.
orthopyroxene	22	0.8	U, B	A	DG, CA				Schmid (1967): Figs. 49, 51
clinopyroxene	1	0.9	U (B, F)	A, R	DG, CA, DC	60, < 20	DC, GS	local posttectonic reaction to biotite	Kruhl & Voll (1978/79)
amphibole	24	0.7	U, B, F	A, R	DC	60, < 20	<u>DC</u>	* and often **	Brodie (1981): Plate 1
garnet	5	0.8	F	E, I, A	CA			kelyphitic reaction rims around	Brodie & Rutter (1985): Plate 2
other	2							mafic minerals	Rutter & Brodie (1988): Fig. 5
PARAGNEISS									
quartz	28	0.8	U, B	R, A	DC	60, < 20	DC	*	This paper: Figs. 7a & 7b
K-feldspar	11	0.8	U (B, F)	A, R	DC, CA	< 30, < 10	<u>DC, GS</u>	*	Schmid (1967): Figs. 36, 37
plagioclase	10	0.6	U (B, F)	A, R	DC, CA	< 30, < 10	<u>DC, GS</u>		Zingg et al. (in press): Fig. 4
garnet	29	1.4	F	E, A	CA	< 20	CA		
biotite	2	0.1	U, B (F)	I	DC, CA	< 20	GS	in pressure shadows & dispersed	
sillimanite	18	0.2	U, B, F	I, A	DC, CA			rarely as new needles	
other	2								

PROTOLITH		POGALLO SHEAR ZONE						b
		porphyroclasts			mylonitic matrix		metamorphism	
rock type & mineral	mode (vol %)	intragranular strain features	grain shape	inferred deformation mechanisms	grain size (µm)	inferred deformation mechanisms	syntectonic reactions in mylonites of the Pogallo line / remarks	references
PARAGNEISS & SCHIST								
quartz	30	U, B	R, A	DC	10 - 60	<u>DC</u>	grain size highly variable	Handy (1987): Fig. 8
plagioclase	21	F, U, B	A, E	DG, CA, DC	< 10	GS, DC	plag → Na-plag + white mica + clinozoisite	This paper: Figs. 7c & 7d
biotite	26	U, B, F	A, I	DG, CA	< 10	<u>GS</u>	biotite → chlorite + white mica	Boriani (1971): Fig. 1
sillimanite	12	U, F, B	I	CA			sillimanite → white mica	Boriani (1971): Fig. 3
muscovite	5	U, F, B	A, I	DG, CA	< 10	<u>GS; GS in clinozoisite & chlorite</u>	fine grained white mica	Handy (1987): Fig. 9
garnet	3	F	E, I	CA			garnet → chlorite + white mica	<u>see also:</u>
staurolite	1	U, F	I	DG, CA			staurolite → white mica	Handy (1987): Fig. 10
other	2							Handy (1986): Chapt. 4 Schilling (1957): Fig. 19 Peyronel Pagliani & Boriani (1962)
METABASITE								
amphibole	48	U, F	I	DG, CA	<10	GS, DC	amphibole → biotite + chlorite	Boriani (1971): Fig. 5
plagioclase	42	U, F	I	DG, CA	<10	GS, DC	plag → Na-plag + white mica + clinozoisite	
quartz	4	U, B	R	DC	10-20	DC		
biotite	3	U, B, F	I	DG, CA	<10	<u>GS; GS in chlorite & clinozoisite</u>	biotite → chlorite	
garnet	1	F	E > I	CA			garnet → chlorite + white mica	
other	2							

Figure 6. Summary of the microstructural characteristics of high-temperature shear zones (a) and the Pogallo shear zone (b), respectively, in the granulite- and amphibolite-facies parts of the Ivrea zone. Intragranular strain features: F, fracture; B, deformation bands, kink bands, or stress twins; U, undulose extinction. Grain shape: I, idiomorphic; E, equidimensional; A, augen shaped; R, ribbon shaped (in order of increasing aspect ratio and strain). Inferred deformation mechanisms: CA, cataclasis; DG, dislocation glide (low-strain crystal plasticity); DC, dislocation creep (high-strain crystal plasticity); GS, viscous grain boundary sliding (dislocation or diffusion accommodated). Underlining indicates the deformation mechanism(s) and mineral(s) that are inferred to govern the bulk flow of the rock (see text for discussion). Features of each mineral are listed in order of decreasing frequency of observation. Parentheses indicate rare occurrence.

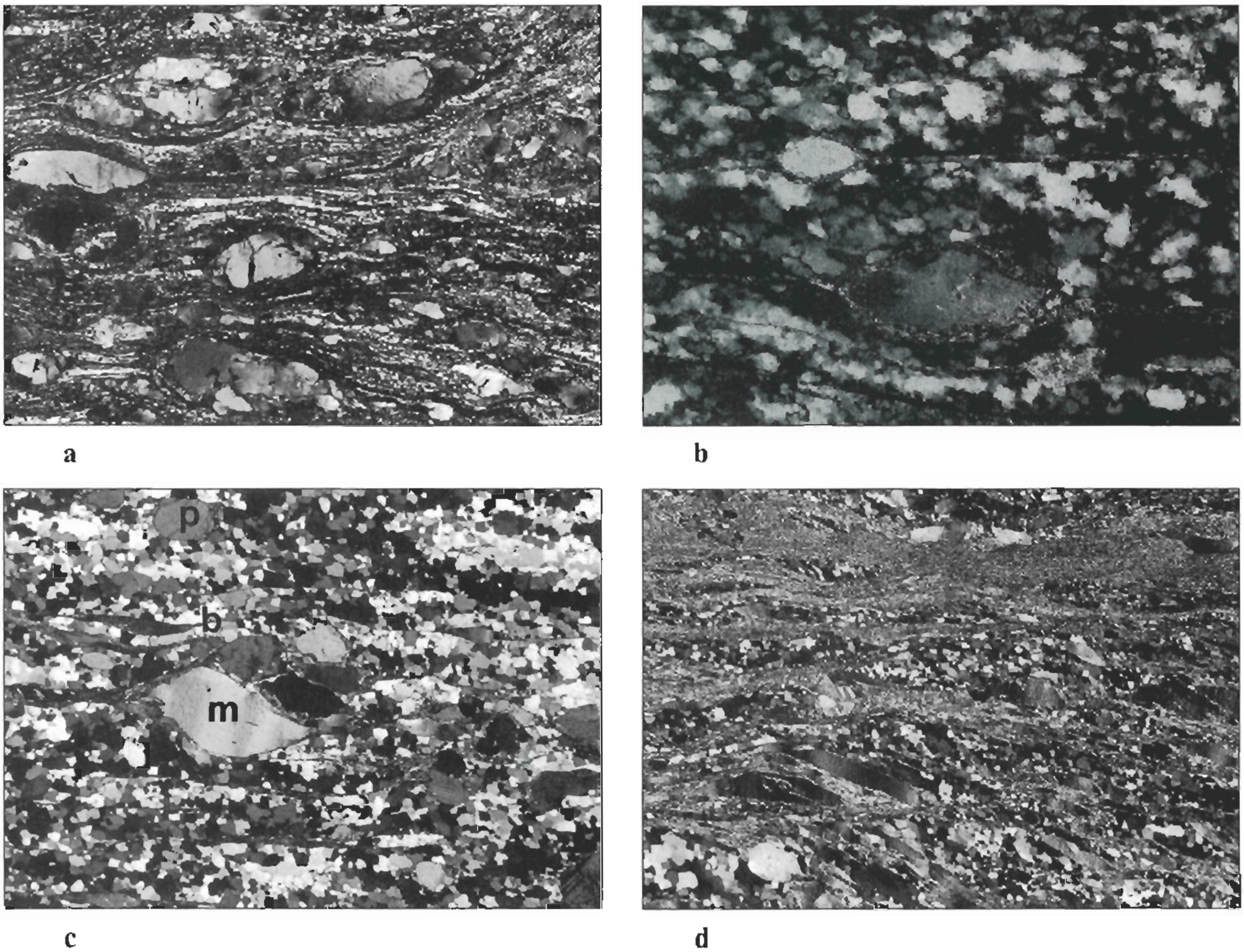

Figure 7. Episode 2 microstructures.

(a) Granulite-facies Ivrea paragneiss mylonitized under upper-amphibolite–facies conditions; matrix comprises dynamically recrystallized quartz, K-feldspar, and plagioclase; elongate boudins of feldspar; equant opaque clasts of garnet (polarized light; frame length, 5.6 mm).

(b) Detailed microstructure of quartz and feldspar in part a; long trains of very fine-grained feldspar grow in the tails of the augen-shaped K-feldspar clasts. Dynamic recrystallization of quartz involves a combination of subgrain rotation and grain boundary migration. See Figure 8, sample Iv-854 for quartz c-axis pattern (polarized light; frame length, 0.7 mm).

(c) Ivrea paragneiss sheared under retrograde amphibolite-facies conditions in the southwest to central part of the Pogallo shear zone (see Fig. 8). Note the bent muscovite clasts (m) and rounded, subequant plagioclase clasts (p) in the dynamically recrystallized quartz matrix. Biotite (b) forms clasts and grows in pressure shadows of all clasts (polarized light; frame length, 11.5 mm).

(d) Greenschist-facies mylonite from the Pogallo line; note transition from a rheology controlled by dynamically recrystallized quartz (bottom) to a rheology governed by a combination of fine-grained syntectonically crystallized white mica + clinozoisite and elongate lenses of dynamically recrystallized quartz (top). (Polarized light; frame length, 5.6 mm.)

crustal section about a subhorizontal rotational axis oriented northeast-southwest (detailed discussion on p. 620–624 in Handy, 1987). When the Pogallo shear zone is restored to its original pre-Alpine orientation, it acquires the configuration of a moderate- to low-angle, southeast-dipping oblique extensional fault that accommodated east-west–directed extension sometime during Late Triassic to Early Jurassic time (Hodges and Fountain, 1984; Handy, 1987).

The viscous creep of quartz is inferred to have controlled bulk flow in the Pogallo shear zone (Fig. 7c). Figure 8 shows that the northwest to southeast decrease in retrograde metamorphic conditions across the shear zone is associated with an overall increase in the volume proportion of subgrain rotation dynamic recrystallization in quartz and a decrease in dynamically recrystallized quartz grain size, especially at the Pogallo line. By analogy with the complete texture analyses of quartzite in Schmid and Casey (1986), the c-axis orientation patterns in Figure 8 indicate that (1) flow within the Pogallo shear zone was highly noncoaxial and involved only a subordinate component of coaxial flattening strain (kinked oblique single-girdle patterns) and (2) hotter syntectonic retrograde conditions

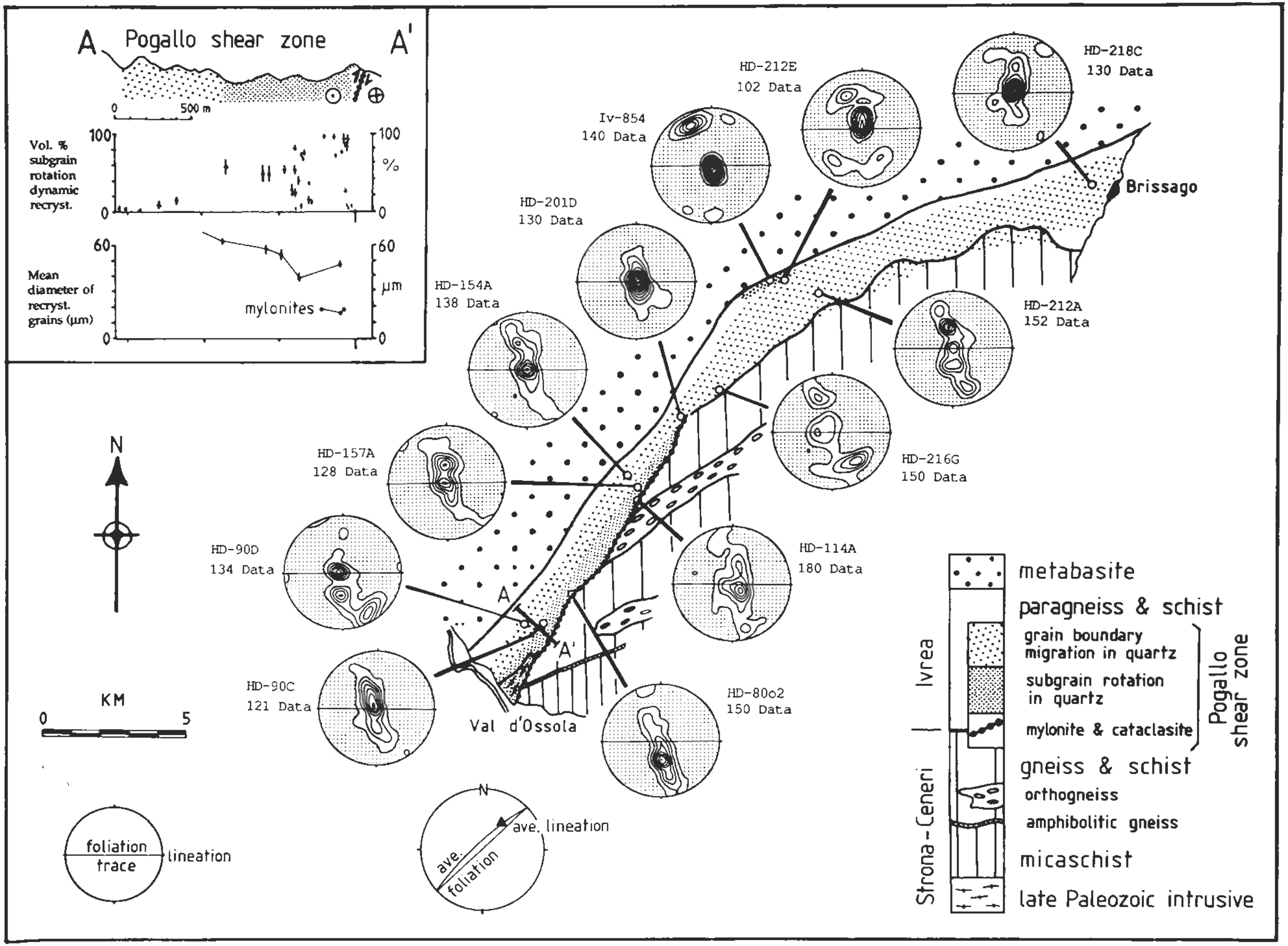

A Pogallo shear zone A'
0 500 m
Vol. % subgrain rotation dynamic recryst.
100
%
0
Mean diameter of recryst. grains (µm)
60
µm
0
mylonites
HD-218C
130 Data
HD-212E
102 Data
Iv-854
140 Data
HD-201D
130 Data
HD-154A
138 Data
HD-157A
128 Data
HD-90D
134 Data
HD-90C
121 Data
HD-212A
152 Data
HD-216G
150 Data
HD-114A
180 Data
HD-80o2
150 Data
Brissago
Val d'Ossola
A
A'
N
KM
0
5
foliation trace
lineation
ave. lineation
ave. foliation
metabasite
paragneiss & schist
grain boundary migration in quartz
subgrain rotation in quartz
mylonite & cataclasite
Pogallo shear zone
gneiss & schist
orthogneiss
amphibolitic gneiss
micaschist
late Paleozoic intrusive
Ivrea
Strona-Ceneri

Figure 8. Quartz c-axis fabrics of the Pogallo shear zone between Val d'Ossola and Brissago (overview in Fig. 1). Inset shows nature of the microstructural transition in quartz from predominantly grain boundary migration to subgrain rotation mechanism of dynamic recrystallization across the Pogallo shear zone between A and A'. Equal-area lower-hemisphere diagrams are contoured at intervals of two times uniform distribution (counting circle = 100/n% of area of projection, where n is number of measurements). Average orientation of mylonitic foliation and mineral-stretching lineation (triangle) in the Pogallo shear zone is shown in equal-area diagram at bottom.

prevailed in the northern and eastern parts of the Pogallo shear zone (point maxima perpendicular to lineation within the foliation plane) than along its contact with the Strona-Ceneri zone (oblique single-girdle patterns).

The development of microstructures and fabrics across and along the Pogallo shear zone reflects overlapping temperature-, time-, and strain-dependent effects during extensional shearing. The distribution of dynamically recrystallized grain size within the Pogallo shear zone indicates that flow stress increased both in the direction of uplift (that is, from northeast to southwest in present coordinates, Fig. 8) and toward the cooler contact with the Strona-Ceneri zone (from northwest to southeast). Discontinuous syntectonic reactions in retrograde greenschist-facies Pogallo mylonites (Fig. 7d) led to a localized reduction in viscosity along the Pogallo line. Cataclastic overprinting within these mylonites (Fig. 10b in Handy, 1987) documents the transition from viscous to frictional behavior. Pogallo shearing occurred at depths of 10 to 15 km and was responsible for thinning ~5 km of crust from the Ivrea-Strona-Ceneri contact (Handy, 1987).

Establishing the relative age of different shearing events in the Ivrea zone is crucial to understanding the crustal-scale rheological evolution of the southern Alpine basement during episode 2. Unfortunately, there is no direct evidence of whether Pogallo shearing is broadly synchronous or much younger than the high-temperature mylonitization in deeper levels of the Ivrea zone. The maximum duration of Pogallo shearing was about 30 m.y., based on knowledge of the maximum displacement (~20 km of offset of the Strona-Ceneri amphibolite band in Fig. 1), the minimum width of the Pogallo shear zone (1 km), and the minimum shear strain rate ($\sim 10^{-13}$ s^{-1}) estimated from syntectonic quartz microstructures (Handy, 1986). This is much less than the 100-m.y. interval (280 to 180 Ma) of rapid cooling in the Ivrea zone indicated by the temperature-time curves in Figure 4 and suggests that high-temperature shearing, which exhumed the deep crust, was diachronous during Early Permian to Early Jurassic time.

We propose that the early and late stages of episode 2 shearing occurred under similar kinematic conditions in the Ivrea zone, but reflect distinctive regional tectonic regimes in the southern Alps (reconstruction will be shown in Fig. 11). Extensional shearing of the Ivrea zone began already in late Paleozoic time (Handy, 1986, 1987; Brodie and Rutter, 1987) and may be genetically linked to basic to intermediate magmatism and the formation of elongate, east-northeast-west-southwest-oriented basins in the upper crust of the southern Alps. The shape and orientation of the basins, the broad range of late Paleozoic magmatic compositions, and the restored, pre-Alpine kinematics in the high-temperature mylonites of the Ivrea zone are all consistent with sinistral transtension of the southern Alpine crust, possibly in a late- to post-orogenic environment of lateral spreading and tectonic escape. Strike-slip tectonics have been proposed for the association of Permo-Carboniferous basins and magmatism in other parts of the Alps (Trümpy, 1982; Mercolli and Oberhänsli, 1988) and western central Europe (Arthaud and Matte, 1975; Ziegler, 1986; Eisbacher and others, 1989). Viewed on a continental scale, these sinistral transtensional faults and basins in the southern Alps may have been conjugate to large dextral strike-slip faults within a broader zone of right-lateral shear between Africa and Europe during Permo-Carboniferous time (Arthaud and Matte, 1975). Such conjugate fault systems are observed in central France (Massif Central) and western Spain, areas where part of the proto-African plate is believed to have indented the proto-European plate (Matte, 1986). The discrepancy in radiometric temperature-time curves for the Ivrea and Strona-Ceneri zones in the vicinity of the Pogallo line indicates that about 3 km of crust was thinned at the Ivrea-Strona-Ceneri contact between Early Permian and Middle Triassic time (Handy, 1987). Brodie and Rutter (1987) estimated that the high-temperature shear zones in metabasic rocks of the Ivrea zone are responsible for an additional 2 km of thinning of the lower crust. Later, Pogallo deformation in the Ivrea zone is kinematically related to the opening of north-northeast-south-southwest-trending, asymmetrical rift basins in the upper crust beginning in the Middle Triassic and accelerating during Late Triassic to Early Jurassic time (Bernoulli, 1964; Kälin and Trümpy, 1977; Bertotti, 1990). Extensional shearing of the deep crust continued in the quartz-rich paragneisses into Early Jurassic time when temperatures in the Ivrea zone fell to below ~300 °C (Figs. 4a and 4b) and deformation along the Pogallo line switched from mylonitic to cataclastic. The locally high paleogeothermal gradient manifested by the syntectonic microstructures and mineral assemblages of the Pogallo shear zone indicates that retrograde middle- to upper-amphibolite-facies conditions persisted in the lower crustal parts of the Ivrea zone during the early stages of Pogallo shearing. Amphibolite-facies annealing in some mylonitized metabasite and peridotite (Fig. 6a) suggests that episode 2 shearing in these deeper crustal rocks stopped earlier than in the relatively weak paragneisses and schists. The similarity of stretching lineation orientations and sense-of-shear directions in the Pogallo shear zone and in high-temperature mylonite zones (Brodie and Rutter, 1987; Handy, 1987) is therefore attributed to the kinematic coincidence of deep-crustal shearing regimes during late Paleozoic east-northeast-west-southwest sinistral transtension and Triassic to Early Jurassic, east-west-directed Tethyan rifting (diagrams and equal-area projections will be shown in Figs. 11a and 11b).

Emplacement Tectonics (Episode 3)

A system of major faults and related brittle folds collectively forms a broad hinge zone that separates uplifted steeply dipping parts of the Ivrea and Strona-Ceneri basement units from their Permian-Mesozoic sedimentary cover to the south and east (Cremosina, Val Cuvia, Pogallo, Lago Maggiore, and Lugano-Grona lines in Fig. 1). These faults are inherited late Paleozoic and early Mesozoic structures (Bernoulli, 1964; Kälin and Trümpy, 1977; Bertotti, 1990) that were reactivated as brittle thrust and/or strike-slip faults during the Alpine orogeny. The abrupt changes in biotite ages among basement blocks separated by reverse faults and thrusts (Fig. 4d) manifest differential uplift, rotation, and fragmentation of the originally deeper levels of the Ivrea crustal cross section. Locally, faulting and associated hydrothermal activity have led to a partial resetting of a few of the biotite ages, particularly along the Insubric line (some of the 120- to 170-m.y. ages in Figs. 4c and 4d).

Regarded on the scale of the Alps, the arcuate shape of the Ivrea zone and the episode 3 fault movement pattern in Figure 1 reflect transpressional tectonics at a restraining bend of the Insubric line, where the main part of the Adriatic plate (southern Alps) indented both the European plate (Penninic units) and marginal fragments of the Adriatic plate (Austro-Alpine units; Laubscher, 1971; Schmid and others, 1989). In detail, the kinematic history of episode 3 faulting in Figure 1 is very complex (Schumacher, 1990; area east of Lago Maggiore) and is related to several Alpine tectonic events: (1) Late Cretaceous and/or Paleocene thrusting and uplift, possibly associated with pre-late Eocene, south-

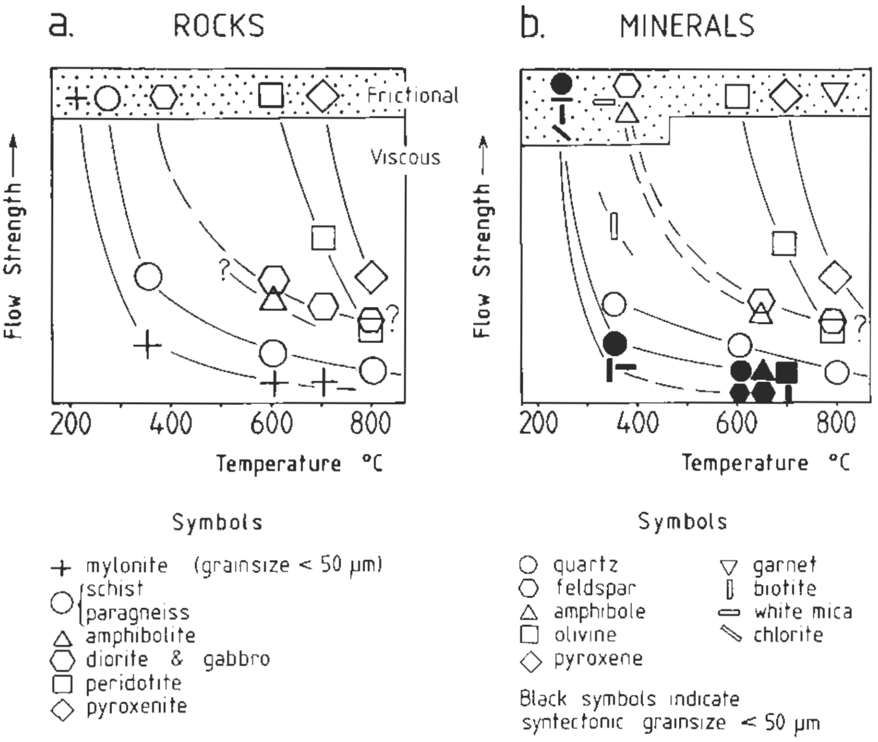

Figure 9. Diagrams of creep strength versus temperature for rocks (a) and minerals (b) in the Ivrea zone based on observations in Figures 3, 5, 6, and 7 and the criteria discussed in the text.

vergent thrusting farther to the east in the Adamello region of the southern Alps (Brack, 1981); (2) late Eocene to early Oligocene thrusting, evidenced by Oligocene conglomerates of the southern Alpine molasse that include components of upper Eocene limestone (Bernoulli and others, 1989); (3) Oligocene to Miocene transpressional Insubric tectonics, involving south-vergent thrusting and dextral strike slip (Schmid and others, 1987, 1989); and (3) early or late Miocene thrusting, observed at the contact between Mesozoic and Tertiary cover rocks south of the Lago Lugano (Fig. 1; Bernoulli and others, 1989). Due to the relatively discrete nature of brittle deformation, Alpine faulting has not greatly altered the older internal structural and metamorphic features of the exhumed lower crust, nor has it seriously disrupted the original depth sequence of crustal levels presently exposed in the area of Figure 1. Because displacements along the major strike-slip faults (for example, Cremosina line) are poorly constrained, however, the amount of lateral offset between the subvertical Ivrea–Strona–Ceneri basement section and its sedimentary cover is unknown.

COMPARATIVE RHEOLOGY OF ROCKS AND MINERALS DEFORMED IN THE DEEP CRUST

Curves of creep strength versus temperature for naturally deformed rocks and mineral aggregates shown in Figure 9 are derived from observations of episode 1 and 2 structures reviewed above. These semiquantitative diagrams are valid for the full range of strain rates estimated for natural viscous creep of silicate rocks at depth (10^{-10} and 10^{-14} s^{-1}), although most of the creep-strength curves stem from observations in high-strain-rate (10^{-10}–10^{-12} s^{-1}) shear zones. Temperature is estimated from the syntectonic mineral assemblages and geothermometry, whereas the relative strengths among naturally deformed rocks and minerals are approximated from the meso- and microstructural criteria outlined above.

There is good agreement between the inferred relative strengths of naturally deformed rocks and the relative creep strengths reported for experimentally deformed monomineralic aggregates (for example, Carter and Tsenn, 1987). Quartz-rich rock is weaker than feldspathic and amphibolitic rocks. Metabasite is approximately equal in strength to peridotite at very high temperatures, but is weaker than peridotite toward lower temperatures. Generally, the relative flow strength among rocks and minerals increases with decreasing temperature, reflecting the trends of increasing stress and strain partitioning during crustal cooling. Isothermal variations and inversions in the relative strength of naturally deformed rocks and minerals shown in Figure 9 indicate the importance of strain-dependent reductions in grain size on the rheology. Grain size reduction in experimentally deformed rock is associated with a marked strength drop at constant strain rate, especially if the grain size is sufficiently small for dislocation- and diffusion-accommodated grain boundary sliding mechanisms to become rate competitive with intracrystalline plasticity (Etheridge and Wilkie, 1979; Schmid, 1982).

The microstructural observations above indicate that approximating the flow strength of polymineralic rocks by extrapolating experimental flow laws for monomineralic aggregates to natural strain rates is justifiable for a wide range of crustal compositions and conditions. In many rocks, one mineral is inferred to control the bulk rheology and shows microstructural evidence of dislocation creep (Handy, 1990). In mylonite with a uniformly fine grain size and in some rock deformed at very high homologous temperatures, however, two or more minerals deforming by diffusion creep and/or dislocation creep are inferred to have controlled viscous flow together (Fig. 6). Using experimental monomineralic flow laws for one of the constituent minerals to estimate the strength of such rocks is not strictly valid, but probably does not lead to significant over- or underestimates of rock strength if the mineral strength contrasts are less than an order of magnitude. By far the largest source of uncertainty is the propagation of experimental error associated with the extrapolation of experimental flow laws from laboratory to natural strain rates (Paterson, 1987). What should clearly be avoided is the extrapolation of laboratory creep laws for polymineralic rocks in which the constituent minerals have strength contrasts

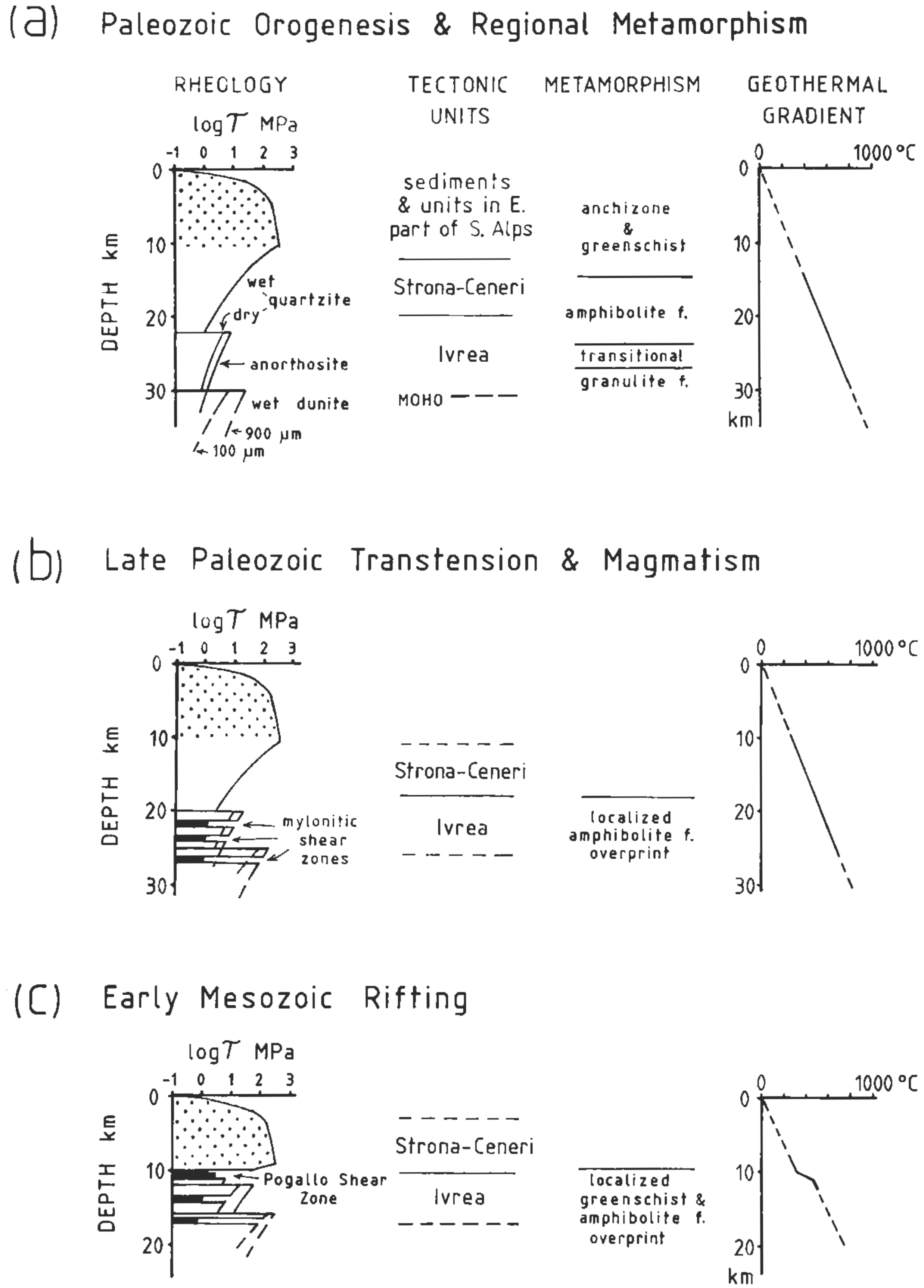

Figure 10. Profiles of shear strength versus depth for the Ivrea crustal cross section in the Val d'Ossola section during (a) episode 1 and (b and c) the two stages of episode 2. Geothermal gradients are estimated (solid lines) and interpolated (dashed lines) from petrological and radiometric data (see text).

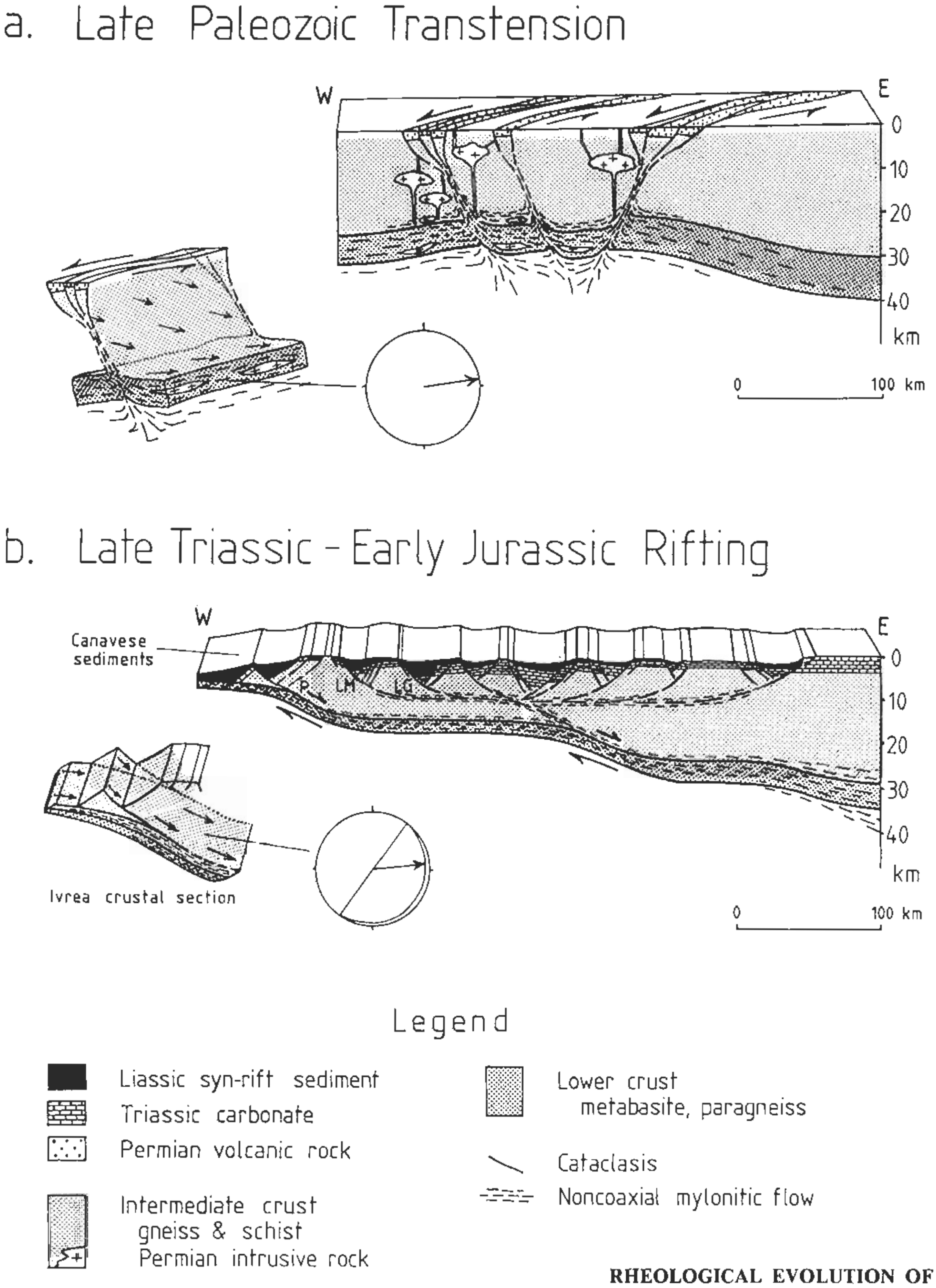

Figure 11. Reconstruction of the southern Alpine continental crust during the two stages of episode 2 crustal shearing: (a) late Paleozoic transtension and (b) Late Triassic to Early Jurassic rifting. Upper crustal basinal geometry and thicknesses in b are modified from Bernoulli and others (1979). Equal-area diagrams depict the average pre-Alpine orientation of episode 2 stretching lineations (arrows) and foliation in the high-temperature shear zones (from Brodie and Rutter, 1987, and our own data) and the Pogallo shear zone (from Handy, 1987). Symbols: P, Pogallo shear zone; LM, Lago Maggiore line; LG, Lugano-Grona line. See Figure 1 for present map location of these structures.

of an order of magnitude or greater at experimental or natural strain rates. Extrapolating creep laws from experimental to natural conditions entails assuming that either stress or strain rate is homogeneous on the grain scale. This results in significant under- or overestimates of bulk creep strength, especially for rocks with high volume percentages (≥70%) of very strong minerals (discussion in Handy, 1990).

RHEOLOGICAL EVOLUTION OF THE SOUTHERN ALPINE CRUST

Figure 10 contains a sequence of profiles of strength versus depth through the Ivrea-Strona-Ceneri basement section and its upper crustal cover during episodes 1 and 2 shown in Figure 2. These profiles are constructed for a combination of Mohr-Coulomb frictional sliding and intracrystalline, power-law creep at an assumed average crustal shear strain rate of 10^{-14} s^{-1} (see Meissner and Strehlau, 1982, for details of construction). The temperature-depth profiles in the righthand column of Figure 10 are derived from the mineral parageneses, geothermometry, and radiometric age determinations in the Ivrea and Strona-Ceneri zones (reviews in Zingg, 1983; Zingg and others, 1991).

The monomineralic aggregates used to model viscous creep in Figure 10 are chosen in accordance with the microstructural observations above (Fig. 6) showing which minerals controlled the creep behavior in each compositional domain of the Ivrea–Strona-Ceneri basement section; hydrous quartzite (Jaoul and others, 1984) represents the rheology of upper and intermediate crustal gneiss and schist in the Strona-Ceneri zone and the Ivrea zone, whereas anhydrous quartzite (Jaoul and others, 1984) and anorthosite (Shelton and Tullis, 1981) simulate the flow of granulite-facies paragneiss and feldspathic metabasite in the lower crustal part of the Ivrea zone. Lower crustal metabasite bearing less than 20 vol. % feldspar is rare in the Ivrea zone (Schmid, 1967), and so is rheologically insignificant on the crustal scale. Two dunite creep laws (Chopra and Paterson, 1981) are used to represent the creep of hydrous peridotite (grain sizes of 100 and 900 μm) in the lower crust and the upper mantle originally underlying the Ivrea crustal cross section. Values of the frictional constants are from Byerlee's (1978) compilation of experimental data for a wide range of crustal rocks. These frictional constants are valid to effective pressures of about 1,500 MPa in most crystalline rocks (Stesky, 1978). In the absence of good constraints on pore-pressure gradients in the lithosphere, effective pressure in the frictional sliding regime is assumed equal to lithostatic pressure (that is, pore pressure = 0). There is microstructural evidence of localized synmylonitic pore-pressure cycling and stick-slip behavior at the transition from viscous creep to frictional sliding in some mylonites of the Pogallo line (Fig. 4.20 in Handy, 1986), but for the sake of simplicity, such transient effects are not included in our model (see, however, Etheridge and others, 1984). Deformation is assumed to be simple shear in the triaxial stress state ($\sigma_1 > \sigma_2 = \sigma_3$). This formulation is used because most large-strain structures in the Ivrea crustal cross section were originally horizontal to subhorizontal at depth.

During Paleozoic deformation (episode 1), strain in the lower and intermediate crust is homogeneously distributed on the crustal scale owing to the low strength contrasts among rocks and minerals. This strain distribution implies that regional stress levels were at least as high as the creep strength of peridotite and pyroxenite, the strongest rocks in the crustal section. The experimentally predicted strength contrasts across the crust-mantle transition in Figure 10a are too large to account for the homogeneous distribution and style of episode 1 deformation in the Ivrea zone. This discrepancy is due partly to the assumption of a constant regional strain rate for all lithological layers, which maximizes estimates of strength contrast at lithological boundaries. In addition, the syntectonic olivine grain size in the upper mantle may have been smaller than that of the experimentally deformed dunite used here (100–900 μm) and observed in strongly annealed Ivrea peridotite (~2 mm). Small grain size enhances impurity weakening in silicates through diffusion and/or microcracking at the grain boundaries and promotes grain-size–sensitive creep mechanisms (for example, Jaoul and others, 1984).

Overall cooling and decompression during episode 2 lithospheric extension led to a marked contrast in the deformational behavior of the different crustal levels as stress and strain were concentrated within mylonitic shear zones (black layers in Figs. 10b and 10c). During late Paleozoic time, transtensional faulting and basin formation in the upper crust and high-temperature shearing in the deep crust (Ivrea zone) were accommodated by dilation and magmatism, especially in the intermediate crustal Strona-Ceneri zone (Early Permian granite and volcanic and volcaniclastic rocks in Fig. 1). Triassic to Early Jurassic rifting involved brittle extensional faulting of the upper and intermediate crust and retrograde shearing in the lower crust and basal part of the intermediate crust. The correlation of retrograde amphibolite- to greenschist-facies mylonitization with rapid cooling in the Ivrea zone at a time when the Strona-Ceneri zone was already cool (Fig. 4) is consistent with the interpretation that the hot lower crust was uplifted with respect to the intermediate crust during extension.

The contrasting orientation of episode 1 folds in the Ivrea and Strona-Ceneri zones described earlier probably reflects the partitioning of episode 2 strain into the Ivrea zone as well as the aforementioned differences in the episode 1 tectonometamorphic histories of the two basement units. In the deeper and hotter Ivrea zone, episode 2 shearing is interpreted to have partly rotated episode 1 fold axes into their current northeast-southwest–trending orientation, subparallel to the shearing direction indicated by the northeast-plunging mineral stretching lineations in mylonites. The originally cooler Strona-Ceneri zone is largely unaffected by penetrative episode 2 shearing, and episode 1 folds retained their widely varied orientations. Therefore, the oldest structural and metamorphic features are best preserved in the intermediate crust.

The potential significance of such localized shearing for passive margin structure is shown in Figure 11b. Our reconstruction of the southern Alpine crustal configuration in the early Mesozoic locates the Ivrea–Strona-Ceneri basement section at or near the base of the rapidly thinning neck of the continental crust. Shear zones in the lower crust and at the base of the intermediate crust acted as decoupling horizons between the intermediate to upper crust and upper mantle. The foundering of the southern Tethyan continental margin during Late Triassic and Early Jurassic time involved the development of asymmetrical basins bounded by listric faults with opposite dip directions (Fig. 11b; Bernoulli and others, 1979; Winterer and Bosellini, 1981). This upper crustal extensional configuration may reflect conjugate low-angle master faults at depth (Fig. 11b) that initially accommodated bulk coaxial shear of the continental margin. The subsequent westward shift in the locus of rapid sedimentation at the end of Early Jurassic time suggests that rifting of the southern Tethyan continental margin migrated toward the eventual ocean-spreading axis (Gaetani, 1975; Winterer and Bosellini, 1981). This is inferred to have been coupled with a westward increase in the component of bulk noncoaxial shear as strain was increasingly accommodated within one of the conjugate master faults. Stepwise crustal delamination (Lister and others, 1986) of the distal (western) part of the southern Alpine continental margin occurred along large zones of noncoaxial shear like the Pogallo shear zone (Fig. 11b) that became more diffuse with depth toward the continent before transferring extensional strain from the crust into the mantle. The continentward dip of large shear zones in the lower crust and of most brittle faults bounding asymmetrical basins in the western part of the upper southern Alpine crust is compatible with the idea that extensional faulting in the upper and intermediate crust propagated across the eventual spreading axis of the Tethyan ocean (see Le Pichon and Barbier, 1987). This geometry ultimately resulted in the thinning out of the intermediate crust in highly attenuated, distal parts of the rifted, southern Tethyan continental margin (Fig. 11b). Such a Mesozoic extensional configuration provides an alternative to Alpine transpressional tectonics as a way of bringing pre- and synrift Canavese sediments of the southern Alps into their present contact with deep crustal rocks of the Ivrea zone (Figs. 1 and 11b).

DISCUSSION AND CONCLUSIONS

The high-strain rheology of the southern Alpine continental crust is very sensitive to changing physical conditions of deformation (especially temperature) and to the location and orientation of inherited structures. Strength contrasts between intermediate to lower crustal rocks and upper mantle rocks in the Ivrea crustal cross section are inferred to be low at the natural strain rates, high temperatures, and high pressures of Paleozoic regional metamorphism. If interlayered ultrabasic and metabasic rocks in the originally deepest levels of the Ivrea zone are considered to represent the pre-Alpine Moho (Fountain, 1976; Hale and Thompson, 1982), then the similar style and orientation of Paleozoic folds in these rocks suggests that the continental Moho was not a significant mechanical discontinuity, at least during Paleozoic orogenesis.

Penetrative viscous flow during late Paleozoic and early Mesozoic crustal attenuation is localized within the lower crust and within quartz-rich rocks at the base of the intermediate crust (Ivrea zone). The latter rocks were sheared during both Paleozoic and early Mesozoic times and represent a major detachment horizon within the southern Alpine crust. Higher levels of the intermediate crust (Strona-Ceneri zone) are largely unaffected by extensional flow, and so preserve the older structures and metamorphism better than do deeper crustal levels. Mylonitic shear zones are ubiquitous and equally well developed in all rock types of the Ivrea zone, suggesting that rheological instabilities that developed during shearing (for example, as the result of syntectonic mineral reactions) were at least as important in localizing strain as were instabilities that arose from pre-existing compositional and lithological inhomogeneities.

The localization of stress and strain into large shear zones within the crust is similar to the much smaller-scale concentration of stress and strain into the weakest mineral(s) of a polymineralic rock (Handy, 1990). By analogy, anastomosing mylonitic shear zones are inferred to control the high-strain rheology of the crust, even though they make up a relatively small proportion (10%–20% by volume) of the crustal section. Because the viscosity of such fine-grained shear zones is significantly below that of the adjacent less- or undeformed rocks, lithospheric strength is probably considerably less than that predicted in many rheological models which assume only power-law dislocation creep at constant strain rate, grain size, crustal structure, and thermal gradient.

Finally, how are big pieces of lower continental crust like the Ivrea zone uplifted and deformed without being completely overprinted? The theoretical rheological concept of "whole lithosphere failure" or WLF (Kuznir and Park, 1986) predicts that large horizontal strains are possible only after flow stresses exceed the yield strength of all rocks and the entire lithosphere deforms either by dislocation creep or frictional sliding. Clearly this is inconsistent with the preservation of old structures and mineral assemblages between mylonitic shear zones, indicating that flow stresses only locally exceeded yield strength. A more plausible explanation for the zonation of fabrics of different ages about shear zones is that increasing stress concentration within shear zones during progressive strain localization was accompanied by rapid stress relaxation in those parts of shear zones that became inactive during localization. Future studies aimed at reconstructing the stress history of crustal-scale fault zones may provide the conceptual basis for more sophisticated modeling of lithospheric rheology.

ACKNOWLEDGMENTS

Throughout the long evolution of this paper, we have benefited from fruitful discussions with many colleagues, especially G. Bertotti, D. Bernoulli, J. Hunziker, S. Schmid, M. Schumacher, E. Rutter, and K. Brodie. A. Bürgi and U. Klötzli kindly gave us a preprint of their manuscript. D. Fountain and M. Casey are thanked for constructive reviews that clarified our thinking on and exposition of several important points. This project was supported by grants from the Swiss National Science Foundation (2971-0.88 to M.H. and 2000-005654 to A.Z.)

REFERENCES CITED

Arthaud, F., and Matte, Ph., 1975, Les décrochements tardi-hercyniens du sud-ouest de l'Europe. Géometrie et essai de reconstitution des conditions de la déformation: Tectonophysics, v. 25, p. 139–171.

Barazangi, M., and Brown, L., eds., 1986, Reflection seismology: A global perspective: American Geophysical Union Geodynamics Series, v. 13, 311 p.

Behrmann, J. H., and Mainprice, D., 1987, Deformation mechanisms in a high-temperature quartz-feldspar mylonite: Evidence for superplastic flow in the lower continental crust: Tectonophysics, v. 140, p. 297–305.

Bernoulli, D., 1964, Zur Geologie des Monte Generoso (Lombardische Alpen): Beiträge zur Geologischen Karte der Schweiz (Neue Folge), v. 118, 134 p.

Bernoulli, D., Caron, C., Homewood, P., Kalin, O., and van Stuijvenberg, J., 1979, Evolution of continental margins in the Alps: Schweizerische Mineralogische und Petrographische Mitteilungen, v. 59, p. 165–170.

Bernoulli, D., Bertotti, G., and Zingg, A., 1989, Northward thrusting of the Gonfolite Lombarda ("South-Alpine Molasse") onto the Mesozoic sequence of the Lombardian Alps: Implications for the deformation history of the southern Alps: Eclogae Geologicae Helvetiae, v. 82, no. 3, p. 841–856.

Bertotti, G., 1990, The deep structure of the Monte Generoso basin: An extensional basin in the South-Alpine Mesozoic passive continental margin: Mémoires Société Géologique de France, v. 156, p. 303–308.

Biot, M. A., 1964, Theory of internal buckling of a confined multilayered structure: Geological Society of America Bulletin, v. 75, p. 563–568.

Boriani, A., 1971, Blastomylonites and recrystallized mylonites: Rendiconti Società Italiana di Mineralogia e Petrologia, v. 27, p. 35–47.

Boriani, A., and Origoni Giobbi, E., 1984, High-grade regional metamorphism, anatexis, degranitization and the origin of the granites: An example from the South-Alpine basement, *in* Proceedings of the 27th International Geological Congress: Moscow, U.S.S.R., VNU Science Press, v. 9, p. 41–66.

Boriani, A., and Sacchi, R., 1973, Geology of the junction between the Ivrea-Verbano and Strona-Ceneri zones (southern Alps): Memorie degli Instituti di Geologia e Mineralogia, Università di Padova, v. 28, p. 1–35.

Boriani, A., Bigioggero, B., and Origoni Giobbi, E., 1977, Metamorphism, tectonic evolution and tentative stratigraphy of the "Serie dei Laghi," geological map of the Verbania area (northern Italy): Memorie di Scienze Geologiche, Università di Padova, v. 32, p. 1–26.

Boriani, A., Colombo, A., and Macera, P., 1985, Radiometric geochronology of the central Alps: Rendiconti Società Italiana di Mineralogia e Petrologia, v. 40, p. 139–186.

Boullier, A. M., and Gueguen, Y., 1975, SP-mylonites. Origin of some mylonites by superplastic flow: Contributions to Mineralogy and Petrology, v. 50, p. 93–104.

Brace, W. F., and Kohlstedt, D. L., 1980, Limits on lithospheric stress imposed by laboratory experiments: Journal of Geophysical Research, v. 85, p. 6248–6252.

Brack, P., 1981, Structures in the southwestern border of the Adamello Intrusion (Alpi Bresciane, Italy): Schweizerische Mineralogische und Petrographische Mitteilungen, v. 61, no. 1, p. 37–50.

Brodie, K. H., 1980, Variations in mineral chemistry across a shear zone in phlogopite peridotite: Journal of Structural Geology, v. 2, p. 265–272.

—— 1981, Variation in amphibole and plagioclase composition with deformation: Tectonophysics, v. 78, p. 385–402.

Brodie, K. H., and Rutter, E. H., 1985, On the relationship between deformation and metamorphism with special reference to the behaviour of basic rocks, *in* Thompson, A. B., and Rubie, D. C., eds., Metamorphic reactions: Kinetics, textures and deformation (Advances in physical geochemistry, Volume 4): New York, Springer-Verlag, p. 138–179.

—— 1987, Deep crustal extensional faulting in the Ivrea zone of northern Italy: Tectonophysics, v. 140, p. 193–212.

Bürgi, A., and Klötzli, U., 1990, New data on the evolutionary history of the Ivrea zone (northern Italy): Swiss Association of Petroleum Geologists and Engineers Bulletin, v. 56, no. 130, p. 49–70.

Byerlee, J., 1978, Friction of rocks: Pure and Applied Geophysics, v. 116, p. 615–626.

Carter, N. L., 1976, Steady state flow of rocks: Reviews of Geophysics and Space Physics, v. 14, p. 301–360.

Carter, N. L., and Tsenn, M. C., 1987, Flow properties of continental lithosphere: Tectonophysics, v. 136, p. 27–63.

Cassinis, G., Mattavelli, L., and Morelli, G. L., 1978, Studio petrografico e mineralogico delle formazione di Collio nel Permiano inferiore nell'alta Val Trompia (Prealpi Bresciane): Memoria Società Geologica, Università di Padova, v. 32, p. 1–13.

Chopra, P. N., and Paterson, M. S., 1981, The experimental deformation of dunite: Tectonophysics, v. 42, p. 75–110.

Eisbacher, G. H., Lüschen, E., and Wickert, F., 1989, Crustal-scale thrusting and extension in the Hercynian Schwarzwald and Vosges, central Europe: Tectonics, v. 8, no. 1, p. 1–21.

Etheridge, M. A., and Wilkie, J. C., 1979, Grain size reduction, grain boundary sliding and the flow strength of mylonites: Tectonophysics, v. 58, p. 159–178.

Etheridge, M. A., Wall, V. J., and Cox, S. F., 1984, High fluid pressures during regional metamorphism and deformation: Implications for mass transport and deformation mechanisms: Journal of Geophysical Research, v. 89, p. 4344–4358.

Fountain, D. M., 1976, The Ivrea-Verbano and Strona-Ceneri zones, northern Italy: A cross-section of the continental crust—New evidence from seismic velocities of rock samples: Tectonophysics, v. 33, p. 145–165.

—— 1986, Implications of deep crustal evolution for seismic reflection interpretation, *in* Barazangi, M., and Brown, L., eds., Reflection seismology: The continental crust: American Geophysical Union Geodynamics Series, v. 14, p. 1–7.

Gaetani, M., 1975, Jurassic stratigraphy of the southern Alps, *in* Squyres, C. H., ed., Geology of Italy (Volume 1): Tripoli, Libya, Earth Sciences Society of the Libyan Arabic Republic, p. 377–402.

Garuti, G., and Friolo, R., 1978/79, Textural features and olivine fabrics of peridotites from the Ivrea-Verbano zone (Italian western Alps): Memorie di Scienze Geologiche, Università di Padova, v. 33, p. 111–125.

Hale, L. D., and Thompson, G. A., 1982, The seismic reflection character of the continental Mohorovicic discontinuity: Journal of Geophysical Research, v. 87, p. 4625–4635.

Handy, M. R., 1986, The structure and rheological evolution of the Pogallo fault zone, a deep crustal dislocation in the southern Alps of northwestern Italy (Prov. Novara) [Ph.D. dissert.]: Basel, Switzerland, University of Basel, 327 p.

—— 1987, The structure, age and kinematics of the Pogallo fault zone, southern Alps, northwestern Italy: Eclogae Geologicae Helvetiae, v. 80, p. 593–632.

—— 1990, The solid-state flow of polymineralic rocks: Journal of Geophysical Research, v. 95, p. 8647–8661.

Hodges, K. V., and Fountain, D. M., 1984, Pogallo line, south Alps, northern Italy: An intermediate crustal level, low-angle normal fault?: Geology, v. 12, p. 151–155.

Hurford, A. J., 1986, Cooling and uplift patterns in the Lepontine Alps, south central Switzerland, and an age of vertical movement on the Insubric fault line: Contributions to Mineralogy and Petrology, v. 92, p. 413–427.

Jaoul, O., Tullis, J., and Kronenberg, A., 1984, The effect of varying water content on the behavior of Heavitree quartzite: Journal of Geophysical Research, v. 89, p. 4298–4312.

Jordan, P. G., 1987, The deformational behaviour of bimineralic limestone-halite aggregates: Tectonophysics, v. 135, p. 185–197.

Kälin, O., and Trümpy, D. M., 1977, Sedimentation und Paläotektonik in den westlichen Südalpen: Zur triasisch-jurassischen Geschichte des Monte Nudo-Beckens: Eclogae Geologicae Helvetiae, v. 70, p. 295–350.

Kirby, S. H., 1980, Tectonic stresses in the lithosphere: Constraints provided by the experimental deformation of rocks: Journal of Geophysical Research, v. 85, p. 6353–6363.

—— 1983, Rheology of the lithosphere: Reviews of Geophysics and Space Physics, v. 21, p. 1458–1487.

Knipe, R. J., 1989, Deformation mechanisms—Recognition from natural tectonites: Journal of Structural Geology, v. 11, no. 1/2, p. 127–146.

Kruhl, J. H., and Voll, G., 1976, Fabrics and metamorphism from the Monte Rosa root zone into the Ivrea zone near Finero, southern margin of the Alps: Schweizerische Mineralogische und Petrographische Mitteilungen, v. 56, p. 627–633.

—— 1978/79, Deformation and metamorphism of the western Finero Complex: Memorie di Scienze Geologiche, Università di Padova, v. 33, p. 95–109.

Kuznir, N. J., and Park, R. G., 1986, Continental lithosphere strength: The critical role of lower crustal deformation, *in* Dawson, J. B., Carswell, D. A., Hall, J., and Wedepohl, K. H., eds., The nature of the lower continental crust (Geological Society Special Publication, Volume 24): Oxford, England, Blackwell, p. 77-93.

Laubscher, H. P., 1971, Das Alpen-Dinariden Problem und die Palinspastik der südlichen Tethys: Geologische Rundschau, v. 60, p. 813–833.

Le Pichon, X., and Barbier, F., 1987, Passive margin formation by low-angle faulting within the upper crust: The northern Bay of Biscay margin: Tectonics, v. 6, p. 133-150.

Lister, G. S., Etheridge, M. A., and Symonds, P. A., 1986, Detachment faulting and the evolution of passive continental margins: Geology, v. 14, p. 246–250.

Matte, Ph., 1986, Tectonics and plate tectonics model for the Variscan belt of Europe: Tectonophysics, v. 126, p. 329–374.

Meissner, R., and Strehlau, J., 1982, Limits of stresses in continental crusts and their relation to the depth-frequency distribution of shallow earthquakes: Tectonics, v. 1, p. 73–89.

Mercolli, I., and Oberhänsli, R., 1988, Variscan tectonic evolution in the central Alps: A working hypothesis: Schweizerische Mineralogische und Petrographische Mitteilungen, v. 68, p. 491–500.

Mooney, W. D., and Brocher, A. B., eds., 1987, Special issue on deep seismic reflection profiling of the continental lithosphere: Royal Astronomical Society Geophysical Journal, v. 89, no. 1, 447 p.

Ord, A., and Christie, J. M., 1984, Flow stresses from microstructures in mylonitic quartzites of the Moine thrust zone, Assynt area, Scotland: Journal of Structural Geology, v. 6, p. 639-654.

Paterson, M. S., 1987, Problems in the extrapolation of laboratory rheological data: Tectonophysics, v. 133, p. 33-43.

Peyronel Pagliani, G., and Boriani, A., 1962, Miloniti e cataclasiti al limite fra "zona dioritico-kinzigitica" e "zona Strona orientale" nella bassa Val d'Ossola e loro significato tettonico: Rendiconti Società di Mineralogica Italiana, v. 18, p. 137–156.

Pinarelli, L., Del Moro, A., and Boriani, A., 1988, Rb-Sr geochronology of Lower Permian plutonism in Massicio dei Laghi, southern Alps (NW-Italy): Rendiconti Società Italiana di Mineralogia e Petrologia, v. 43, p. 411–428.

Ramberg, H., 1964, Selective buckling of composite layers with contrasted rheological properties; a theory for simultaneous formation of several orders of folds: Tectonophysics, v. 1, p. 307-341.

Ramsay, J. G., 1967, Folding and fracturing of rocks: New York, McGraw-Hill, 568 p.

Ranalli, G., and Murphy, D. C., 1987, Rheological stratification of the lithosphere: Tectonophysics, v. 132, p. 281–295.

Rutter, E. H., and Brodie, K. H., 1988, The role of tectonic grain size reduction in the rheological stratification of the lithosphere: Geologische Rundschau, v. 77, p. 295-308.

Schilling, J., 1957, Petrographisch-geologische Untersuchungen in der unteren Val d'Ossola: Schweizerische Mineralogische und Petrographische Mitteilungen, v. 37, p. 435-544.

Schmid, R., 1967, Zur Petrographie und Struktur der Zone Ivrea-Verbano zwischen Valle d'Ossola und Val Grande (Prov. Novara, Italien): Schweizerische Mineralogische und Petrographische Mitteilungen, v. 47, p. 935–1117.

Schmid, R., and Wood, B. J., 1976, Phase relationships in granulitic metapelites from the Ivrea-Verbano zone (northern Italy): Contributions to Mineralogy and Petrology, v. 54, p. 255–279.

Schmid, S. M., 1982, Microfabric studies as indicators of deformation mechanisms and flow laws operative in mountain building, *in* Hsü, K. J., ed., Mountain building processes: London, England, Academic Press, p. 95–110.

Schmid, S. M., and Casey, M., 1986, Complete texture analysis of commonly observed quartz c-axis patterns, *in* Hobbs, B. E., and Heard, H. C., eds., Mineral and rock deformation studies (Paterson Volume): American Geophysical Union Monograph, v. 36, p. 263–286.

Schmid, S. M., Zingg, A., and Handy, M. R.,1987, The kinematics of movements along the Insubric line and the emplacement of the Ivrea zone: Tectonophysics, v. 135, p. 47-66.

Schmid, S. M., Aebli, H. R., Heller, F., and Zingg, A., 1989, The role of the Periadriatic line in the tectonic evolution of the Alps, *in* Coward, M. P., Dietrich, D., and Park, R. G., eds., Alpine tectonics: Geological Society of London Special Publication, v. 45, p. 153–171.

Schumacher, M., 1990, Alpine basement thrusts in the eastern Seengebirge: Eclogae Geologicae Helvetiae, v. 83, no. 3 (in press).

Shelton, G., and Tullis, J., 1981, Experimental flow laws for crustal rocks [abs.]: Eos (American Geophysical Union Transactions), v. 62, no. 17, p. 396.

Sibson, R. H., 1982, Fault zone models, heat flow, and the depth distribution of earthquakes in the continental crust of the United States: Seismological Society of America Bulletin, v. 72, p. 151–163.

——— 1983, Continental fault structure and the shallow earthquake source: Geological Society of London Journal, v. 140, p. 741–767.

Sills, J. D., and Tarney, J., 1984, Petrogenesis and tectonic significance of amphibolites interlayered with metasedimentary gneisses in the Ivrea zone: Southern Alps, northwest-Italy: Tectonophysics, v. 107, p. 187-206.

Smith, R. B., and Bruhn, R. L., 1984, Intraplate extensional tectonics of the eastern Basin-Range: Inferences on structural style from seismic reflection data, regional tectonics, and thermal-mechanical models of brittle-ductile deformation: Journal of Geophysical Research, v. 89, p. 5733-5762.

Steck, A., and Tièche, J. C., 1976, Carte géologique de l'antiforme péridotitique de Finero avec des observations sur les phases de déformation et de recristallisation: Schweizerische Mineralogische und Petrographische Mitteilungen, v. 56, p. 501-512.

Stesky, R. M., 1978, Rock-friction effect of confining pressure, temperature, and pore pressure: Pure and Applied Geophysics, v. 116, p. 690-704.

Trümpy, R., 1982, Alpine paleogeography: A reappraisal, *in* Hsü, K. J., ed., Mountain building processes: London, England, Academic Press, p. 149–156.

Tullis, J. A., 1979, High temperature deformation of rocks and minerals: Reviews of Geophysics and Space Physics, v. 17, p. 1137-1154.

Wagner, G. A., Reimer, G. M., and Jäger, E., 1977, Cooling ages derived by apatite fission track, mica Rb/Sr and K/Ar dating: The uplift and cooling history of the central Alps: Memorie di Scienze Geologiche, Università di Padova, v. 30.

Walter, P., 1950, Das Ostende des basischen Gesteinszuges Ivrea-Verbano und die angrenzenden Teile der Tessiner Wurzelzone: Schweizerische Mineralogische und Petrographische Mitteilungen, v. 30, p. 1-144.

Winterer, E. L., and Bosellini, A., 1981, Subsidence and sedimentation on Jurassic passive continental margin, southern Alps, Italy: American Association of Petroleum Geologists Bulletin, v. 65, p. 394-421.

Ziegler, P. A., 1986, Geodynamic model for the Paleozoic crustal consolidation of western and central Europe: Tectonophysics, v. 126, p. 303–328.

Zingg, A., 1980, Regional metamorphism in the Ivrea zone (southern Alps, N-Italy): Field and microscopic investigations: Schweizerische Mineralogische und Petrographische Mitteilungen, v. 60, p. 153-179.

——— 1983, The Ivrea and Strona-Ceneri zones (southern Alps, Ticino and northern Italy): A review: Schweizerische Mineralogische und Petrographische Mitteilungen, v. 63, p. 361-392.

Zingg, A., Handy, M. R., Hunziker, J. C., and Schmid, S. M., 1990, Tectonometamorphic history of the Ivrea zone and its relationship to the crustal evolution of the southern Alps: Tectonophysics (in press).

MANUSCRIPT RECEIVED BY THE SOCIETY JUNE 30, 1989
REVISED MANUSCRIPT RECEIVED JUNE 5, 1990
MANUSCRIPT ACCEPTED JUNE 21, 1990